

Interacting dynamical systems on networks and fractals: discrete and continuous models, mean-field limit, and convergence rates

Georgi S. Medvedev*

February 2, 2026

Abstract

We develop a continuum limit and mean-field theory for interacting particle systems (IPS) on self-similar networks, a new class of discrete models whose large-scale behavior gives rise to nonlocal evolution equations on fractal domains. This work extends the graphon-based framework for IPS, used to derive continuum and mean-field limits in the non-exchangeable setting, to situations where the spatial domain is fractal rather than Euclidean. The motivation arises from both physical models naturally formulated on fractals (e.g., heterogeneous media and fractal scattering) and real-world networks exhibiting hierarchical or quasi-self-similar structure.

Our analysis relies on tools from fractal geometry, including Iterated Function Systems (IFS) and self-similar measures. A central result is an explicit isomorphism between self-similar IPS and graphon IPS, which allows us to justify the continuum and mean-field (Vlasov-type) limits in the self-similar setting. This connection reveals that macroscopic dynamics on fractal domains emerge naturally as limits of dynamics on appropriate discretizations of fractal sets.

Another contribution of the paper is the derivation of optimal convergence rates for the discrete self-similar models. We introduce a scale of generalized Lipschitz spaces on fractals, extending the Nikolskii-Besov spaces used in the Euclidean setting, and obtain convergence estimates for discontinuous Galerkin approximations of nonlocal equations posed on fractal domains. These results apply to kernels with minimal regularity addressing models relevant in applications, including discontinuous singular kernels arising in acoustic scattering on fractal screens.

Finally, we interpret self-similar networks as Galerkin discretizations of nonlocal problems on fractal sets connecting our results to numerical analysis of PDEs on fractal domain. On the other hand, this work fits into the broader effort to extend the classical PDEs to fractal domains, which holds significant potential for both theoretical advances and numerical exploration.

2020 *Mathematical Subject Classification.* 34C15, 28A80, 37M15, 92B20.

Keywords and phrases. Interacting particle system, self-similar network, continuum limit, mean-field limit, rate of convergence, martingale, isomorphism, graphon, fractal, Sierpinski Gasket, Galerkin method, Kuramoto model

*Department of Mathematics, Drexel University, 3141 Chestnut Street, Philadelphia, PA 19104, medvedev@drexel.edu

1 Introduction

By an interacting particle system (IPS), we understand a differential equation model describing the evolution of a large ensemble of particles, whose dynamics is governed by the combination of intrinsic forces acting on individual particles and pairwise interactions with other particles according to specified rules. Examples include gases composed of many molecules moving under the laws of classical mechanics and interacting through gravitational forces, plasmas where ions and electrons interact via electrostatic potentials, as well as neuronal networks where neurons interact by means of synaptic currents, to name a few [76, 43, 49].

When the size of the system is large enough, the long time asymptotic behavior in such systems often can be understood by considering a continuum (thermodynamic) limit as the size of the system goes to infinity. If the system contains random initial data or random parameters, its macroscopic behavior can be captured by the the Vlasov equation, a PDE describing the evolution of the distribution of particles in the phase space. The derivation of the Vlasov equation in the *exchangeable* setting when all particles are statistically identical dates back to the works by Dobrushin and Neunzert [32, 76, 43]. Modern applications of dynamical networks in biology and social sciences, such as neuronal networks, flocking and swarming models, opinion dynamics, and consensus protocols, as well as in the models of technological systems like the Internet and power grids, feature spatially structured interactions. The pattern of interactions is determined by a graph or rather a system of graphs. Such systems are *non-exchangeable*. The derivation of the Vlasov equation in this case takes into account the information about how these graphs behave as the system size grows.

The approach to deriving the continuum limit and Vlasov equations for non-exchangeable IPS on convergent graph sequences was developed in [64, 65, 67, 53]. The key new ingredient in the derivation of the limiting equations for the IPS on networks is the use of graphons, measurable functions that represent graphs and limit points of graph sequences [62]. This graphon-based framework has since been successfully applied in a variety of contexts, including coupled oscillator models [19, 20, 22, 21, 68, 25, 26], models of interacting diffusions [63, 27, 7], optimal control [40], mean-field games [17, 3], neuronal networks [50], epidemic spread [4], and image processing [44] among others. In addition, related techniques have been developed for other types of graph limit representations [42, 41].

In this paper, we likewise develop the continuum limit for IPS evolving on self-similar networks. Our motivation for studying dynamics on self-similar structures is twofold. First, Euclidean geometry does not always adequately capture disordered heterogeneous materials such as porous media, rocks, foams, and certain biological tissues, which exhibit irregular, statistically self-similar patterns [13, 6]. In the context of networks, the hierarchical organization of certain networks, including the Internet, infectious disease networks, and the dendritic trees of certain neurons, can be modelled by self-similar graphs approximating fractals. While self-similarity in real-world networks is rarely exact in the strict mathematical sense, self-similar graphs remain valuable for exploring its influence on network behavior - just as classical random graph models (e.g., Erdős–Rényi, small-world, or power-law graphs) are employed to study the role of topology in dynamical systems [22, 25].

Conversely, there are physical models that are readily expressed as nonlocal equations on a fractal domain, and one might be interested in methods for numerical integration of such models. The discrete networks analyzed in this paper can be interpreted as Galerkin approximations of the continuous models on fractal domains. In this context, the results in Section 7 establish convergence of the discontinuous Galerkin

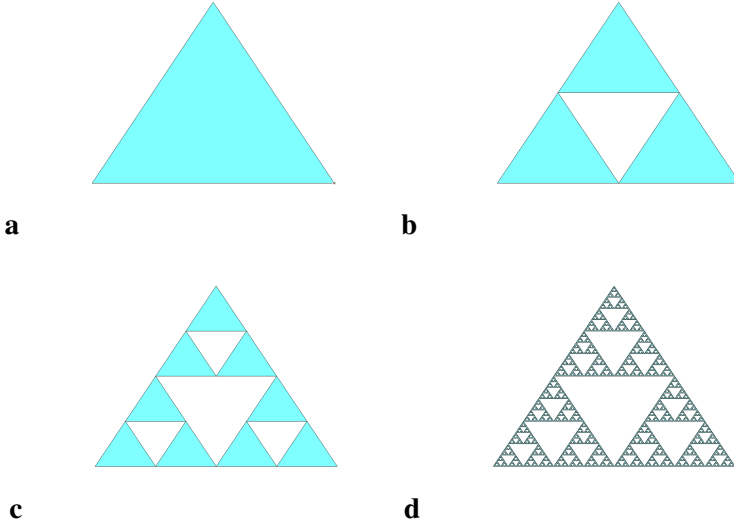


Figure 1: **a, b, c**) Three consecutive prefractals. **d)** SG.

method.

To study the speed of convergence, we introduce a scale of normed spaces of integrable functions on fractals, which imitate generalized Lipschitz spaces [31, Chapter 2, § 9], also known as Nilokskii-Besov spaces [9]. A related scale of Besov-type spaces was used in [51]. Our rate of convergence estimates extend the results for the discontinuous Galerkin method for problems on Euclidean domains analyzed in [54] to the fractal setting. The results in Section 7 are optimal in the sense that they reflect the generalized Lipschitz regularity of the graph limit given by the kernel $W \in L^1(K, \mu)$.

A prototypical example of a nonlocal model posed on a fractal domain is the acoustic scattering problem for a fractal screen, which reduces to the integral equation (cf. [14])

$$\int_{\Gamma} \Phi(x, y) \psi(y), d\mathcal{H}^d(y) = g(x), \quad x \in \Gamma. \quad (1.1)$$

Here, \mathcal{H}^d denotes the d -dimensional Hausdorff measure on the d -set Γ , Φ is the fundamental solution of the Helmholtz equation, and the right-hand side g is selected from an admissible class ensuring the solvability of (1.1) (see [14] for details).

A central component in determining the convergence rate of the discontinuous Galerkin method for (1.1) is the estimation of the error incurred by approximating a function by its L^2 -projection onto a finite-dimensional space of piecewise constant functions [15, 16]. Section 7 develops such estimates for a broad class of self-similar domains, providing the foundation for Galerkin schemes on fractal domains.

In addition to the applications outlined above, there is another compelling reason to study self-similar networks. We show that dynamical models on self-similar graphs lead to equations for macroscopic dynamics on fractal domains. This, in turn, emphasizes a different suite of tools needed to characterize the

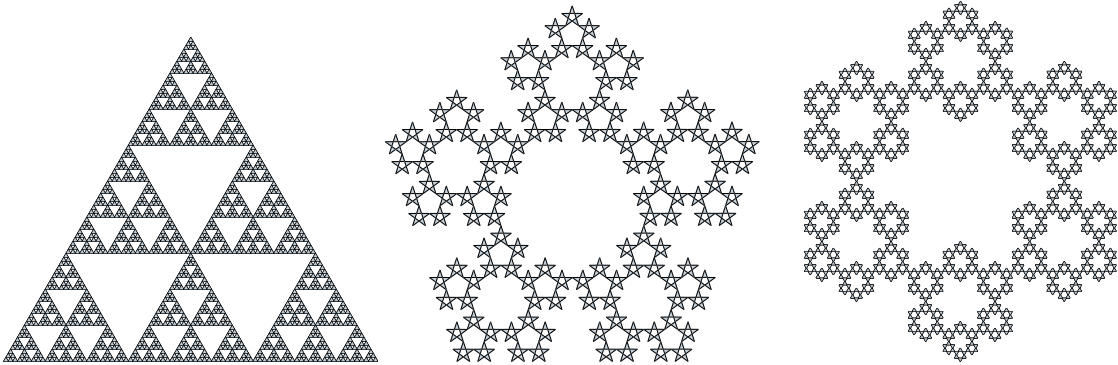


Figure 2: Examples of attractors of IFS: the three-level SG, SG_3 , the pentagasket, and the hexagasket (see [79] for more details).

convergence of the discrete models to the continuum limit. While the analysis of graphon dynamical systems features the spaces of graphons and the properties of the cut norm [64, 65, 67, 53, 35], the analysis of self-similar networks, on the other hand, requires the setting of the symbolic (shift) space associated with Iterated Function Systems (IFS) [47], self-similar measures, and fractal dimension, indispensable in the analysis on fractals [37, 5, 8]. In this respect, the continuum limit theory for IPS on self-similar networks extends and complements the theory for graphon dynamical systems. It gives rise to a new class of models that fits naturally into the broader effort to extend the classical theory of PDEs to fractal domains (see, e.g., [56, 79, 46, 39, 36]), which holds significant potential for both theoretical advances and numerical exploration [74].

At the same time, the present work aligns with a growing trend toward exploring interacting dynamical systems on discrete structures beyond graphs and their limits. For instance, models on hypergraphs, metric graphs, simplicial complexes, and discretizations of Riemannian manifolds have gained attention due to their potential applications in data science and image processing [77, 1, 11]. In a similar spirit, the present work introduces a new class of networks leading to nonlocal equations on fractal domains.

In the next section, we recall the principal results on graphon IPS. These include the continuum limit for IPS on graphs, formulated as a nonlocal nonlinear heat equation and studied in [64, 65, 67], as well as the mean-field (Vlasov) limit, which was rigorously justified in [53]. We then summarize the convergence rate analysis for discrete-to-continuum approximations developed in [54].

The main objective of this paper is to extend these results to IPS defined on self-similar graphs. To prepare for this, we first review the analytical tools from fractal geometry that will be essential in the self-similar setting. As a model of a self-similar network, we choose graphs approximating self-similar sets, which arise as attractors of Iterated Function System (IFS). The topology of the attractors of an IFS is described by the establishing a correspondence with the space of symbolic sequences. The latter is also used to define a measure on the attractor of the IFS. Both ingredients are essential for formulating discrete models on self-similar networks. They are also used in the analysis of the continuum limit and the mean-field limit of the discrete network. In Section 3 we review the IFS and self-similar measures. We also discuss the separation conditions that are used to classify self-similar sets.

After that in Section 4, we introduce a class of self-similar IPSs and state our main results concerning their continuum and mean-field limits. Specifically, we establish the wellposedness of the continuum limit in the form of the nonlocal evolution equation on self-similar domain, write down the Vlasov equation describing the mean-field limit for the IPS at hand and formulate two theorems: one - on the convergence of solutions of discrete models to the continuum limit and the second one - on the convergence of empirical measures to the solution of the initial value problem for the Vlasov equation.

To prove convergence to the continuum limit and to justify the mean-field limit, we use the isomorphism between self-similar sets and the unit interval as well between integrable functions on self-similar sets and those on the unit intervals established in Section 5. We use these relationships to show the correspondence between solutions for self-similar IPS and their graphon counterparts and prove the theorems from the previous section.

We then analyze the convergence rate of self-similar IPS toward their continuum limit in Section 7. The main problem here is to find the right way to describing the regularity of the data in particular the regularity of the kernel of the nonlocal operator, which controls the rate of convergence of the L^2 -projectins onto a subspace of piecewise constant functions. In the Euclidean setting, it was shown in [54] that the generalized Lipschitz spaces provide the desired formalism. The definition of these spaces is based on the L^p -modulus of continuity. In Section 7, we find a way to extend the modulus of continuity to the fractal setting by taking into account the geometry of the fractal domain (see Definition 7.1). Building on this definition, we define generalized Lipschitz spaces for functions on self-similar domains and estimate the rate of convergence of the L^2 -projections in terms of these spaces. This yields the rate of convergence of the discrete models to the continuum limit, or equivalently for the piecewise constant Galerkin method for nonlocal equations on self-similar domains. The implementation of the Galerkin method requires numerical evaluation of integrals for functions on self-similar domains. We review a few ideas that can be used to that effect and formulate the corresponding algorithms in the Appendix. We conclude with a brief discussion in Section 8.

2 Graphon interacting particle systems

2.1 Models and examples

Consider the following IPS

$$\dot{u}_{n,i} = f(t, u_{n,i}) + n^{-1} \sum_{j=1}^n w_{n,ij} D(u_{n,i}, u_{n,j}), \quad i \in [n] \doteq \{1, 2, \dots, n\} \quad (2.1)$$

where $u_{n,i} : \mathbb{R}^+ \rightarrow \mathbb{R}^k$ stands for the state of particle i . Function f defines intrinsic dynamics of particle i . The sum on the right-hand side of (2.1) models the interactions between particles. D is the interaction function.

Throughout this paper, D is a bounded Lipschitz continuous function and f is jointly continuous and Lipschitz continuous in u . These assumptions will be implicitly assumed in all statements below.

Weights

$$w_{n,ij} = n^2 \int_{Q_{n,i}} \int_{Q_{n,j}} W(x, y) dx dy, \quad Q_{n,i} = \left[\frac{i-1}{n}, \frac{i}{n} \right), \quad (2.2)$$

are derived from a given graphon $W \in L^\infty([0, 1]^2)$, which determines the limiting connectivity of the network.

Along with (2.1), we consider the following IPS on random graphs:

$$\dot{u}_{n,i} = f(t, u_{n,i}) + n^{-1} \sum_{j=1}^n \xi_{n,ij} D(u_{n,i}, u_{n,j}), \quad i \in [n] \doteq \{1, 2, \dots, n\}. \quad (2.3)$$

Here, we replace the deterministic weights $w_{n,ij}$ with Bernoulli random variables:

$$\mathbb{P}(\xi_{n,ij} = 1) = w_{n,ij} \quad \text{and} \quad \mathbb{P}(\xi_{n,ij} = 0) = 1 - w_{n,ij}. \quad (2.4)$$

For the random network model, we assume that the graphon W is nonnegative and bounded by 1. We also assume that $\xi_{n,ij}$ are independent for $i \neq j$. For undirected graphs, one can first restrict to $1 \leq i < j \leq n$ and then extend to the remaining i and j by symmetry: $\xi_{n,ji} = \xi_{n,ij}$. The deterministic and continuum systems (2.1) and (2.3) share the same continuum limit [64, 67].

Remark 2.1. *The sign of $\xi_{n,ij}$ in (2.3) determines the type of interactions. Depending on the modeling formalism, negative sign may correspond to repulsive vs attractive coupling in coupled oscillator models [23], or antiferromagnetic vs ferromagnetic coupling in spin models [2]. One can extend (2.3) to allow for interactions of both types (cf. [67, Equation (2.17)]). To this end, let $W = W^+ - W^-$, where nonnegative W^+ and W^- are the positive and negative parts of W respectively. Then one can define weights separately for W^+ and W^- :*

$$w_{n,ij}^\pm = n^2 \int_{Q_{n,i}} \int_{Q_{n,j}} W^\pm(x, y) dx dy. \quad (2.5)$$

and

$$\mathbb{P}(\xi_{n,ij}^\pm = 1) = w_{n,ij}^\pm \quad \text{and} \quad \mathbb{P}(\xi_{n,ij}^\pm = 0) = 1 - w_{n,ij}^\pm. \quad (2.6)$$

Finally, replace the the coupling term in (2.3) by two sums as follows

$$\dot{u}_{n,i} = f(t, u_{n,i}) + n^{-1} \left\{ \sum_{j=1}^n \xi_{n,ij}^+ D(u_{n,i}, u_{n,j}) - \sum_{j=1}^n \xi_{n,ij}^- D(u_{n,i}, u_{n,j}) \right\}, \quad i \in [n]. \quad (2.7)$$

The continuum limit of (2.7) is derived exactly in the same way as that for (2.3), and, therefore, we focus on the latter model.

Example 2.2. (cf. [66]) Let $0 \leq p, r \leq 1/2$ and define

$$W(x, y) = \begin{cases} 1-p, & \min\{|x-y|, 1-|x-y|\} \leq r, \\ p, & \text{otherwise.} \end{cases} \quad (2.8)$$

The band structure of W is shown in Figure 3a. Plots b and c illustrate the structure of the deterministic weighted network (2.2) and random graph (2.4). The latter is called a small-world graph.

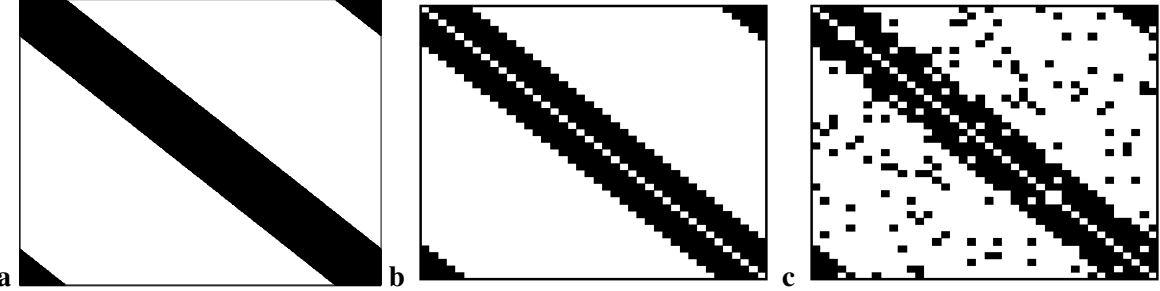


Figure 3: **a** W takes values $1 - p$ and p over the black and white regions respectively. **b, c** Pixel plots of the deterministic weighted network (2.2) and random graph (2.4).

Additional parameters can be easily incorporated into (2.1) or (2.3). For the former model, this can be done as follows:

$$\dot{u}_{n,i} = f(t, u_{n,i}, \lambda_i) + n^{-1} \sum_{j=1}^n w_{n,ij} D(u_{n,i}, u_{n,j}), \quad (2.9)$$

$$\dot{\lambda}_i = 0, \quad \lambda_i \in \mathbb{R}^p, \quad i \in [n]. \quad (2.10)$$

Equation (2.1) covers many interesting models in nonlinear science. We discuss a few representative examples below.

Example 2.3. We start with the Kuramoto model of coupled phase oscillators (cf. [60, 19, 68]):

$$\begin{aligned} \dot{u}_i &= \omega_i + \frac{K}{n} \sum_{j=1}^n a_{ij} \sin(2\pi(u_j - u_i)), \\ \dot{\omega}_i &= 0, \quad i \in [n], \end{aligned} \quad (2.11)$$

Here, $u_i : \mathbb{R}^+ \rightarrow \mathbb{T} \doteq \mathbb{R}/\mathbb{Z}$ is the phase of oscillator $i \in [n]$, $K \in \mathbb{R}$ is the coupling strength. The adjacency matrix (a_{ij}) defines the connectivity of the network. The intrinsic frequencies ω_i , which may be random, are assigned through the initial condition.

The Kuramoto model plays an important role in the theory of synchronization. With $\omega_i = 0$ Equation (2.11) has been used to study relaxation dynamics of the XY-model in statistical physics [28].

Example 2.4. If inertia and damping are included into the Kuramoto model, we obtain the following model

$$\begin{aligned} \dot{u}_i &= v_i \\ \dot{v}_i &= -\gamma v_i + \omega_i + \frac{K}{n} \sum_{j=1}^n a_{ij} \sin(2\pi(u_j - u_i)), \\ \dot{\omega}_i &= 0, \quad i \in [n]. \end{aligned}$$

Although the phase space of each oscillator is two-dimensional (three-dimensional for the augmented model), the continuum and the mean-field limits for (2.4) are derived exactly in the same way as for the scalar Kuramoto model in (2.3) (cf. [21, 25]). A variant of this model appears in statistical physics under the name of Hamiltonian mean-field model [61].

Example 2.5. *The following model appears in the literature in the various contexts including opinion dynamics and consensus protocols*

$$\dot{u}_i = \frac{1}{n} \sum_{j=1}^n a_{ij} D(u_j - u_i), \quad i \in [n],$$

where $u_i \in \mathbb{R}$ quantifies the tendency of agent i to support a certain opinion and D is interaction function, which could be and identity map in the basic or a more elaborate version as for example in the Krauss-Hegselmann bounded confidence model [45].

Other examples include the Cucker–Smale model [29], power networks [33], and the classical N -body problem [75], to name a few. For all such models, when it comes to describing the continuum limit of coupled networks with structured interactions, (2.1) serves as a analytically convenient prototypical system.

2.2 Continuum limit

Pathwise analysis of (2.1) is often not feasible for large n , leading one to seek a macroscopic description of the collective dynamics of (2.1). Below we explain three types of results concerning the description of discrete systems (2.1) and (2.3) in the limit as $n \rightarrow \infty$.

We will start our discussion of the continuum limit of (2.1) and (2.3) with the following nonlinear heat equation

$$\partial_t u(t, x) = f(t, u) + \int_{[0,1]} W(x, y) D(u(t, x), u(t, y)) dy, \quad x \in [0, 1]. \quad (2.12)$$

Here, the unit interval $[0, 1]$ is the label space as before and graphon $W(x, y)$ describes the limiting connectivity of the network.

Remark 2.6. *We have replaced a large finite-size IPS with a continuum of particles labeled by $x \in [0, 1]$, i.e., the label space is the unit interval equipped with Lebesgue measure. In fact, any Borel probability space can serve as a label space. In practice, it suffices to use the unit interval equipped with Lebesgue measure, since any standard nonatomic probability space is isomorphic to it. In the analysis of self-similar IPS below, we will be led to use a fractal set with the appropriate self-similar measure as the label space.*

The connection between the continuum limit (2.12) and the discrete models (2.1) and (2.3) is explained in the following theorem.

Theorem 2.7. [64, 65] *Let $u(t, x)$ be the solution of the IVP for (2.12) subject to $u(0, \cdot) = g \in L^2([0, 1])$. Likewise,*

$$\begin{aligned} u^n(t, x) &= \sum_{i=1}^n u_{n,i}(t) \mathbf{1}_{Q_{n,i}}(x), \\ \bar{u}^n(t, x) &= \sum_{i=1}^n \bar{u}_{n,i}(t) \mathbf{1}_{Q_{n,i}}(x) \end{aligned}$$

solve the IVPs for (2.1) and (2.3), respectively, and satisfy

$$u_n(0, \cdot) = \bar{u}_n(0, \cdot) = g^n.$$

Then for $v \in \{u^n, \bar{u}^n\}$

$$\|u - v\|_{C(0,T;L^2(Q))} \leq C (\|g - g^n\|_{L^2(Q)} + \|W - W^n\|_{L^2(Q \times Q)}). \quad (2.13)$$

Here, in case $v = \bar{u}^n$ estimate (2.13) holds almost surely with respect the probability measure used in the construction of random graphs (2.4). Recall that the norm in $C(0,T;L^2(Q))$ is defined as follows $\|w\|_{C(0,T;L^2(Q))} \doteq \sup_{t \in [0,T]} \|w(t, \cdot)\|_{L^2(Q)}$.

Remark 2.8. In the case of the model on a random graph (2.3), Theorem 2.7 yields the Strong Law of Large Numbers for the solutions of the IVP across different realizations of the random graph. The Large Deviation Principle is also available [35].

Equation (2.12) was derived and rigorously justified as the continuum limit of (2.1) on dense graphs in [64]. It was later extended to particle systems on random graphs, including sparse random graphs, in [65, 52, 67, 35]. In the case of sparse networks, W must be allowed to be unbounded, for example, $W \in L^1([0, 1]^2)$.

The estimates developed for the justification of the continuum limit (2.12) are also important for the justification of the mean-field limit in the form of the Vlasov equation (2.14), which we will discuss next. Specifically, they are used in the derivation of the Liouville equation, which serves as an important step in derivation of the mean-field limit [53].

Representative applications the continuum limit (2.12) include stability and bifurcations of steady states in particle models on (random) graphs (cf. [66, 72, 73, 69, 70]). The applications of the mean-field limit for (2.1) include synchronization and pattern formation in coupled dynamical systems on graphs (cf. [19, 20, 21, 22, 24, 25]).

2.3 Mean-field limit

Suppose that the discrete models (2.1) and (2.3) are subject to random initial conditions or they contain random parameters. Then the macroscopic behavior of the system in the limit as $n \rightarrow \infty$ is described by the Vlasov equation (cf. [19])

$$\partial_t \rho(t, u, x) + \partial_u \{V(t, u, x)\rho(t, u, x)\} = 0, \quad (2.14)$$

$$V(t, x) = f(t, u) + \int_{[0,1]} \int_{R^k} W(x, y) D(u, v) \rho(t, v, y) dv dy. \quad (2.15)$$

Here, $\rho(t, \cdot, x)$ represents the probability density of the state of particle $x \in [0, 1]$ at time t . As before, we have replaced a large finite-size IPS with a continuum of interacting particles labeled by $x \in [0, 1]$.

If $W \equiv \text{const}$, meaning that every particle interacts with all other particles in the same way, then all particles share the same distribution, and the label $x \in [0, 1]$ is not needed for describing their distribution

in the continuum limit. In this case, (2.1) is referred to as an *exchangeable* system. The mathematical justification of the Vlasov equation in this setting follows from the classical works of Dobrushin [32] and Neunzert [75, 76]. For structured networks, the justification of the Vlasov equation (2.14) was provided in [53] by extending Neunzert's method [75] to the *non-exchangeable* setting (see also [19] for a different approach). Although the analysis in [53] was originally motivated by the Kuramoto model of phase oscillators on graphs, the key ideas developed to address non-exchangeability extend to related models on graphs and other structures (see [42, 58, 59]).

To describe the precise relation between the Vlasov equation and the discrete models (2.1) and (2.3), let $n = m\ell$, $m, \ell \in \mathbb{Z}$, and define the local empirical measure as follows

$$\mathfrak{m}_{m,\ell,t}^x(A) = \frac{1}{\ell} \sum_{j=1}^{\ell} \mathbf{1}_A(u_{n,(i-1)\ell+j}(t)), \quad A \in \mathcal{B}(Q), x \in Q_{m,i}, i \in [m]. \quad (2.16)$$

Here, we first divide $[0, 1]$ into m cells $Q_{m,i}$, $i \in [m]$. Our goal is to construct a piecewise constant (over each $Q_{m,i}$, $i \in [m]$) approximation of the probability distribution of the location particle $x \in Q$ in the phase space at time t , $\mathfrak{m}_{m,\ell,t}^x$. To this end, the number of cells m is chosen sufficiently large so that W^m is sufficiently close to W . Further, each $Q_{m,i}$ is subdivided into ℓ parts. Each part corresponds to a particle in the discrete model (2.1) with $n = m\ell$. The number of parts ℓ must be large enough to achieve a good approximation of the empirical measure $\mathfrak{m}_{m,\ell,t}^x$ for $x \in Q_{m,i}$, for every (fixed) $i \in [m]$. Roughly speaking, particles within each cell $Q_{m,i}$ are treated as identically distributed, because W is approximately constant over each $Q_{m,i} \times Q_{m,j}$. We refer the interested reader to Section 3 in [53] for precise statements and further details.

On the other hand, from the solution of the IVP for the Vlasov equation (2.14) with a given initial condition, we compute

$$\mathfrak{m}_t^x(A) = \int_A \rho(t, x, u) du, \quad A \in \mathcal{B}(Q). \quad (2.17)$$

Note that the local empirical measures $\mathfrak{m}_{m,\ell,t}^x$ are computed from the solutions of the discrete system (2.1), whereas the two-parameter family of measures \mathfrak{m}_t^x is derived from the mean-field limit (2.14). The following theorem details the relationship between the two families of measures and thus clarifies the connection between the Vlasov PDE and the non-exchangeable IPS (2.1).

Theorem 2.9. [53] *For given $\epsilon, T > 0$ and sufficiently large $m, \ell \in \mathbb{N}$, we have*

$$\sup_{t \in [0, T]} \int_Q d_{BL}(\mathfrak{m}_{m,\ell,t}^x, \mathfrak{m}_t^x) dx < \epsilon,$$

provided $\mathfrak{m}_{m,\ell,0}^x$ converge weakly to \mathfrak{m}_0^x for almost every $x \in Q$ as $m, \ell \rightarrow \infty$. Here d_{BL} stands for the bounded Lipschitz distance (cf. [34]).

2.4 Convergence rate

Theorem 2.9 is the second result concerning the continuum description of the IPS (2.1) and (2.3). We now turn to the third result, which addresses the speed of convergence of the discrete models to the continuum

limit. It follows from Theorem 2.7 that the accuracy of approximation of the discrete model by the continuum limit (2.12) depends on the error of approximation of the graphon W by its L^2 -projection W^n . The same is true for the Vlasov equation, albeit it is not explicitly stated in Theorem 2.9. Thus, the rate with which $\|W - W^n\|_{L^2(Q \times Q)}$ tends to zero with $n \rightarrow \infty$ determines the accuracy of the approximation of the discrete models (2.1) and (2.3) by the continuum limit (2.12) and the Vlasov equation (2.14).

It is straightforward to estimate the rate of convergence of $\|W - W^n\|_{L^2(Q \times Q)}$ when W is Hölder continuous [54]. On the other hand, for a graphon W representing the limit of a graph sequence, the natural regularity assumption is measurability or integrability in the case of L^p -graphons with $p \geq 1$ [10]. For $W \in L^p([0, 1]^2)$, it is known that $W^n \rightarrow W$ almost everywhere and in L^p (see, e.g., [18, Proposition 2.6]). However, in the absence of additional assumptions, the convergence may be arbitrarily slow, as the following example from [64] shows.

Example 2.10. Consider $W : [0, 1]^2 \rightarrow \{0, 1\}$ and denote by W^+ and ∂W^+ the support of W and its boundary respectively. Then as was observed in [64]

$$\|W - W^n\|_{L^2([0, 1]^2)}^2 \leq N(\partial W^+, n)n^{-2}, \quad (2.18)$$

where $N(\partial W^+, n)$ is the number of discrete cells $\left[\frac{i-1}{n}, \frac{i}{n}\right) \times \left[\frac{j-1}{n}, \frac{j}{n}\right)$, $i, j \in [n]$, that intersect ∂W^+ .

Let γ stand for the upper box counting dimension $N(\partial W^+, n)$ (cf. [38]),

$$\gamma = \overline{\lim}_{n \rightarrow \infty} \frac{\log N(\partial W^+, n)}{\log n}.$$

Then for any $\epsilon > 0$, we have

$$N(\partial W^+, n) \leq n^{\gamma+\epsilon}. \quad (2.19)$$

By plugging (2.19) into (2.18), we have

$$\|W - W^n\|_{L^2([0, 1]^2)} \leq n^{-1+\frac{\gamma+\epsilon}{2}}. \quad (2.20)$$

The bound on the error of approximation suggests that the convergence can be in principle arbitrarily slow if the upper box counting dimension of the boundary of support of W is sufficiently close to 2.

Thus we are led to the following question: *Under what natural assumptions on W , beyond mere integrability, can one deduce a convergence rate for $W^n \rightarrow W$?* In [54], the authors proposed that the generalized Lipschitz spaces (cf. [78, 31]) provide an appropriate functional framework for this purpose:

$$\text{Lip}(L^p(Q), \alpha) = \{f \in L^p(Q) : \omega_p(f, \delta) \leq C\delta^\alpha\}, \quad 0 < \alpha \leq 1. \quad (2.21)$$

Here, the L^p -modulus of continuity $\omega_p(f, \delta)$ is defined as follows

$$\omega_p(f, \delta) = \sup_{|h| \leq \delta} \|f(\cdot) - f(\cdot + h)\|_{L^p(Q'_h)}, \quad Q'_h = \{x \in Q : x + h \in Q\}, \quad (2.22)$$

and $|x|$ stands for the ℓ^∞ -norm of $x \in \mathbb{R}^d$, and Q is a given domain.

$\text{Lip}(L^p(Q), \alpha)$ is equipped with the norm

$$\|f\|_{\text{Lip}(L^p(Q), \alpha)} = \sup_{\delta > 0} \delta^{-\alpha} \omega_p(f, \delta). \quad (2.23)$$

These spaces play an important role in approximation theory [78, 31] and are closely related to Nikol'skii–Besov spaces, which are used in the analysis of partial differential equations [9].

Lemma 2.11. [54, 71] For $f \in \text{Lip}(L^p([0, 1]^d), \alpha)$,

$$\|f - f^n\|_{L^p([0, 1]^d)} \leq Cn^{-\alpha}. \quad (2.24)$$

Remark 2.12. The proof of Theorem 2.11 in [54] uses a dyadic discretization of $[0, 1]^d$, exploiting the self-similarity of the unit cube. This approach suggests that the approximation result in Lemma 2.11 can be extended to functions in self-similar domains, such as SG. We will address this problem in Section 7.

With Lemma 2.11 in hand, we can refine the convergence estimate in Theorem 2.7 by identifying the exact rate of convergence.

Theorem 2.13. Let $u(t, x)$ be the solution of the IVP for (2.1) subject to $u(0, \cdot) = g \in \text{Lip}(\alpha_1, L^2(Q))$. Suppose further that $W \in \text{Lip}(\alpha_2, L^2(Q \times Q))$. The solutions of the discrete problems u^n and u^n , as described in Theorem 2.7, and $v \in \{u^n, u^n\}$. Then

$$\|u - v\|_{C(0, T; L^2(Q \times Q))} \leq Cn^{-\alpha}, \quad \alpha = \min\{\alpha_1, \alpha_2\}. \quad (2.25)$$

Here, in case $v = u^n$ estimate (4.23) holds almost surely.

3 Background on fractals

In this section, we collect the material from fractal geometry that is necessary for the formulation and analysis of dynamical models on self-similar networks. Specifically, we review the attractors of Iterated Function Systems (IFS) and self-similar measures. The IFS framework was introduced by Hutchinson [47]. Our presentation is based on [5, 8].

3.1 Iterated Function Systems

We begin with the definition of the IFS.

Definition 3.1. Let $\mathcal{F} = \{f_i : \mathbb{R}^d \rightarrow \mathbb{R}^d \mid i \in [k]\}$ be a finite collection of maps such that each f_i is a strict contraction with Lipschitz constant $0 < r_i < 1$, i.e.,

$$|f_i(x) - f_i(y)| \leq r_i |x - y| \quad \text{for all } x, y \in \mathbb{R}^d, \quad i \in [k]. \quad (3.1)$$

Assume that the fixed points of the maps f_i are not all identical, and that each f_i is injective. Then \mathcal{F} is called a contracting IFS.

All results reviewed below hold for IFSs defined on a complete metric space. However, since our motivating examples of fractals are embedded in the Euclidean space, we restrict our attention to \mathbb{R}^d for notational convenience.

In fact, in all examples considered below the contractions are *similitudes*, i.e.,

$$|f_i(x) - f_i(y)| = r_i|x - y| \quad \text{for all } x, y \in \mathbb{R}^d, i \in [k], \quad (3.2)$$

with $0 < r_i < 1$. Nevertheless, since several of the results that follow remain valid under the weaker assumption (3.1), we do not impose (3.2) at this stage.

The contraction mapping principle, applied to the map

$$A \longmapsto \bigcup_{i \in [k]} f_i(A)$$

acting on the space of nonempty compact subsets of \mathbb{R}^d endowed with the Hausdorff metric, implies the existence of a unique compact set K satisfying

$$K = \bigcup_{i \in [k]} f_i(K) \quad (3.3)$$

(cf. [8, Theorem 2.1.1], [47]). The set K is called the *attractor* of the IFS $\mathcal{F} = \{f_i\}_{i \in [k]}$.

If $f_i, i \in [k]$, are similitudes, then the attractor K of the IFS \mathcal{F} is called a *self-similar set*. When no confusion is likely to arise, we sometimes use this term more loosely to refer to attractors of general IFS.

Many canonical examples of fractals, i.e., sets of noninteger Hausdorff dimension, can be realized as self-similar sets. On the other hand, certain regular nonfractal sets, such as the unit cube, also fall within this framework. The fact that the unit cube is a self-similar set is used in Section 5, where we establish an isomorphism between IPS on self-similar sets and those on graphons.

We now present several representative examples of self-similar sets.

Example 3.2. • The Cantor set is the attractor of the following IFS on \mathbb{R} :

$$\{f_1(x) = \frac{x}{3}, f_2(x) = \frac{x}{3} + \frac{2}{3}\}.$$

• The Sierpinski Gasket (SG) is a prototypical example of a planar fractal and is often used as a model domain in the analysis of fractals [56, 79]. We shall frequently refer to it throughout this work. It is the attractor of the following IFS on \mathbb{R}^2 :

$$f_i(x) = \frac{1}{2}(x + v_i), \quad i \in [3], \quad (3.4)$$

where

$$v_1 = (0, 0), \quad v_2 = \left(\frac{1}{2}, \frac{\sqrt{3}}{2}\right), \quad v_3 = (1, 0).$$

• The unit interval is the attractor of the following IFS on \mathbb{R} :

$$f_1(x) = \frac{x}{2}, \quad f_2(x) = \frac{x}{2} + \frac{1}{2}.$$

3.2 Symbolic space

Self-similar sets admit a canonical symbolic representation, which we review in this subsection. It provides a convenient way for analyzing topological and ergodic properties of self-similar sets.

Let

$$\Sigma \doteq [k]^{\mathbb{N}} \quad (3.5)$$

denote set of infinite sequences of k symbols. For each $n \geq 1$, let Σ_n be the set of words of length n , and let

$$\Sigma^* = \bigcup_{n=0}^{\infty} \Sigma_n \quad (3.6)$$

denote the collection of all finite words over $[k]$.

We equip Σ with the metric

$$\rho(i, j) = k^{-|i \wedge j|}, \quad i = (i_1, i_2, \dots), j = (j_1, j_2, \dots),$$

where $i \wedge j$ stands for the common prefix of the two sequences i and j , and $|i \wedge j|$ denotes its length. Thus, $|i \wedge j| = \sup\{l \in \mathbb{N} : i_l = j_l\}$ if $i \wedge j \neq \emptyset$ and 0 otherwise. This metric defines a topology on Σ that is consistent with the product topology. By the Tikhonov's Theorem, (Σ, ρ) is a compact metric space (cf. [5]).

Define the shift map $\sigma : \Sigma \rightarrow \Sigma$ by

$$\sigma(w_1 w_2 w_3 \dots) = w_2 w_3 \dots$$

For each $i \in [k]$, the i th branch of the inverse of σ is given by

$$\sigma_i(w_1 w_2 w_3 \dots) = i w_1 w_2 w_3 \dots \quad (3.7)$$

Each σ_i is a contracting similitude on Σ with Lipschitz constant k^{-1} . Consequently, Σ is a self-similar set with respect to $\{\sigma_i\}_{i \in [k]}$.

We now describe the symbolic representation of K , the self-similar set with respect to $\{f_i\}_{i \in [k]}$. It is provided by the *natural projection* $\pi : \Sigma \rightarrow K$ to be defined below.

For $w = (w_1 \dots w_n) \in \Sigma_n$, denote

$$f_w \doteq f_{w_1} \circ \dots \circ f_{w_n}, \quad K_w \doteq f_w(K).$$

The natural projection is defined by

$$\pi(w) = \bigcap_{n \geq 1} K_{w_1 \dots w_n}, \quad w = (w_1 w_2 \dots) \in \Sigma. \quad (3.8)$$

Since $\{K_{w_1 \dots w_n}\}_{n \geq 1}$ is a nested sequence of compact sets with diameters tending to zero, their intersection consists of a single point. The map π is continuous and surjective (cf. [56, Theorem 1.2.3]). Moreover, for every $i \in [k]$

$$\pi \circ \sigma_i = f_i \circ \pi. \quad (3.9)$$

3.3 Self-similar measures

Measures on a self-similar set K will be defined as pushforwards of Bernoulli measures on the symbolic space. Therefore, we first review the construction of Bernoulli measures.

For $i_1, \dots, i_n \in [k]$, define the cylinders

$$[i_1 i_2 \dots i_n] \doteq \{j = (j_1 j_2 \dots) \in \Sigma : j_l = i_l, 1 \leq l \leq n\}. \quad (3.10)$$

The collection of all cylinders generates the Borel σ -algebra in Σ , $\mathcal{B}(\Sigma)$.

We say that $p = (p_1, p_2, \dots, p_k)$ is a *probability vector*, if

$$p_i > 0 \quad \text{for all } i \in [k], \quad \sum_{i=1}^k p_i = 1.$$

For a given probability vector p , the Bernoulli measure of the cylinders is defined by

$$\mu_p([i_1 i_2 \dots i_n]) = p_{i_1} p_{i_2} \dots p_{i_n}. \quad (3.11)$$

It extends uniquely to a Borel probability measure on $(\Sigma, \mathcal{B}(\Sigma))$. Bernoulli measure μ_p is invariant under the shift map σ (cf. [5]), i.e.,

$$\mu_p(\sigma^{-1}([i_1 i_2 \dots i_n])) = \mu_p([i_1 i_2 \dots i_n]).$$

Furthermore, μ_p is *ergodic*, meaning that for every invariant set $A = \sigma^{-1}(A)$, $\mu_p(A) \in \{0, 1\}$.

Next, let K be an attractor of the IFS \mathcal{F} and consider the pushforward $\nu_p = \pi_* \mu_p$:

$$\nu_p(A) = \mu_p(\pi^{-1}(A)), \quad A \in \mathcal{B}(K). \quad (3.12)$$

The pushforward measure $\nu_p = \pi_* \mu_p$ is the *stationary measure* of the probabilistic IFS (K, \mathcal{F}, ν_p) , which means that

$$\nu_p(A) = \sum_{j=1}^k p_j \nu_p(f_j^{-1}(A)), \quad A \in \mathcal{B}(K). \quad (3.13)$$

The stationary measure is unique [8, Theorem 2.1.1]. If f_i 's are similitudes, ν_p is called a *self-similar measure*.

Assume now that $\{f_i\}_{i \in [k]}$ are similitudes with contraction ratios (r_1, r_2, \dots, r_k) . The *similarity dimension* of K is $s > 0$ such that

$$r_1^s + r_2^s + \dots + r_k^s = 1.$$

The stationary measure corresponding to the probability vector $p = (r_1^s, r_2^s, \dots, r_k^s)$ is called the *natural measure* of the IFS \mathcal{F} . If the Open Set Condition holds, then the Moran–Hutchinson theorem implies that $\dim_H K = s$ and that the natural measure is proportional to the s -dimensional Hausdorff measure restricted to K , namely $c \mathcal{H}^s|_K$ (cf. [8, Theorem 2.2.2]).

We include the definition of the Open Set condition for the reader's convenience.

Definition 3.3. A family of maps $\{f_i\}_{i \in [k]}$ on \mathbb{R}^d satisfies the Open Set Condition if there is a bounded nonempty open set $U \subset \mathbb{R}^d$ such that

$$\begin{aligned} f_j(U) &\subset U, \quad j \in [k], \\ f_i(U) \cap f_j(U) &= \emptyset, \quad i \neq j. \end{aligned}$$

The Open Set Condition says that the overlap of $f_i(K) \cap f_j(K)$ for $i \neq j$ is small. It is one of the separation conditions used to describe the degree of the overlap. All sets in Example 3.2 satisfy the Open Set Condition. For instance, to verify this condition for the SG, one can take the interior of the convex hull of SG. In Section 5, we will formulate a different condition that is more natural for our purposes (see Assumption 5.3). Under the Open Set Condition or under Assumption 5.3, we have the following explicit formula for the pushforward measure ν_p on the cylinders:

$$\nu(K_w) = p_{w_1} p_{w_2} \dots p_{w_n}, \quad \forall w \in \Sigma_n, \quad n \in \mathbb{N}. \quad (3.14)$$

4 Self-similar IPS

4.1 The model

Having reviewed graphon IPS and the necessary background on fractals, we now turn to the formulation of a dynamical model on self-similar networks.

Let K be an attractor of an IFS $\mathcal{F} = \{f_1, f_2, \dots, f_k\}$ equipped with a stationary probability measure ν and consider the following IPS:

$$\dot{u}_w = f(t, u_w) + \sum_{|v|=n} W_{wv} D(u_w, u_v) \nu(K_v), \quad w \in \mathcal{S}^n, \quad (4.1)$$

$$u_w(0) = g_w, \quad w \in \Sigma_n, \quad (4.2)$$

where

$$W_{wv} = \int_{K_{wv}} W(x, y) d(\nu \times \nu)(x, y), \quad g_w = \int_{K_w} g d\nu. \quad (4.3)$$

Throughout, $\int_A f(x) dm(x)$ denotes the average value of f over A , namely

$$\int_A f(x) dm(x) := \frac{1}{m(A)} \int_A f(x) dm(x).$$

$(K_w, w \in \Sigma_n)$ is a self-similar partition of K defined by

$$\mathcal{K}^m \doteq \{K_w : K_w = F_w(K), |w| = m\}, \quad K = \bigcup_{|w|=m} K_w. \quad (4.4)$$

We remind the reader that $F_w \doteq F_{w_1} \circ F_2 \circ \dots \circ F_{w_m}$.

Functions $W \in L^2(K \times K, \nu \times \nu)$, $g \in L^2(K, \nu)$. Further we assume

$$\bar{W} \doteq \max \left\{ \text{ess sup}_{x \in K} \int_K |W(x, y)| d\nu(y), \text{ess sup}_{y \in K} \int_K |W(x, y)| d\nu(x) \right\} < \infty. \quad (4.5)$$

Functions $f(t, u)$ and $D(u, v)$ are jointly continuous and

$$|f(t, u) - f(t, u')| \leq L_f |u - u'|, \quad \forall t \in \mathbb{R}, u, u' \in K, \quad (4.6)$$

$$|D(u, v) - D(u', v')| \leq L_D (|u - u'| + |v - v'|), \quad \forall u, v, u', v' \in K, \quad (4.7)$$

where L_f and L_D are positive Lipschitz constants. In addition,

$$\sup_{K \times K} |D(u, v)| \leq 1. \quad (4.8)$$

It is instructive to compare (4.1) with the IPS on a weighted graph (2.1). Note that the role of the graphon on the unit square is now assumed by W on $K \times K$, where K is an attractor of the IFS \mathcal{F} . The weights (W_{wv}) reflect the nested, possibly fractal, structure of K . This endows the dynamical network model (4.1) with a natural self-similar organization. Hence, Equation (4.1) provides a general framework for modeling self-similar networks.

Remark 4.1. Recall that $[0, 1]$ is the attractor of the IFS $\{f_1(x) = \frac{x}{2}, f_2(x) = \frac{1}{2} + \frac{1}{2}x\}$. Consequently, the model (4.1) contains the graphon IPS (2.1) as a special case. More broadly, self-similar IPS offer a natural and flexible framework for the study of IPS on spaces endowed with hierarchical partitions.

In analogy with (2.12), we expect the following continuum limit for (4.1)

$$\partial_t u(t, x) = f(t, u) + \int_K W(x, y) D(u(t, x), u(t, y)) d\nu(y), \quad (4.9)$$

$$u(0, x) = g(x), \quad x \in K. \quad (4.10)$$

The wellposedness of the IVP (7.4), (4.10) is established by the following theorem.

Theorem 4.2. Suppose (4.5)-(4.8) hold and $g \in L^2(K, \mu)$. Then for any $T > 0$, the IVP (7.4)-(4.10) has a unique solution $u \in C([-T, T]; L^2(K, \mu))$.

Proof. Let $\mathbf{X} \doteq C([-T, T], L^2(K, \mu))$ and consider $\mathbf{M} : \mathbf{X} \rightarrow \mathbf{X}$ defined as follows

$$\mathbf{M}[\mathbf{u}] \doteq \int_K W(\cdot, y) D(\mathbf{u}(\cdot), \mathbf{v}(y)) d\mu(y). \quad (4.11)$$

Equation (7.4) is a nonlinear differential equation on the Banach space \mathbf{X} :

$$\frac{d\mathbf{u}}{dt} = F(t, \mathbf{u}), \quad (4.12)$$

where

$$F(t, \mathbf{u}) \doteq f(t, \mathbf{u}) + M[\mathbf{u}]. \quad (4.13)$$

In view of (4.6), to show that the right-hand side of (4.13) is Lipschitz continuous in \mathbf{u} , we only need to verify that $M[\mathbf{u}]$ is Lipschitz continuous. To this end, let $\|\cdot\|$ stand for the norm in $L^2(K, \mu)$ and note

$$\begin{aligned} \|\mathbf{M}[\mathbf{u}] - \mathbf{M}[\mathbf{v}]\| &\leq \left\| \int_K |W(\cdot, y)| |D(\mathbf{u}(\cdot), \mathbf{u}(y)) - D(\mathbf{u}(\cdot), \mathbf{u}(y))| d\mu(y) \right\| \\ &\leq L_D \left\| \int_K |W(\cdot, y)| |\mathbf{u}(\cdot) - \mathbf{v}(\cdot)| d\mu(y) \right\| \\ &\quad + L_D \left\| \int_K |W(\cdot, y)| |\mathbf{u}(y) - \mathbf{v}(y)| d\mu(y) \right\| \\ &\leq L_D \bar{W} \|\mathbf{u} - \mathbf{v}\| + L_D \left\| \left(\int_K W(\cdot, y)^2 d\mu(y) \right)^{1/2} \|\mathbf{u} - \mathbf{v}\| \right\| \\ &\leq L_D (\bar{W} + \|W\|_{L^2(K \times K, \mu \times \mu)}) \|\mathbf{u} - \mathbf{v}\|. \end{aligned}$$

The statement of the theorem now follows from a standard result on existence and uniqueness of solutions of initial value problems for differential equations in Banach spaces (cf. [30, Theorem 1.2; Chapter VII]). \square

4.2 Galerkin discretization

We want to show that (7.4) is the continuum limit of the self-similar IPS (4.1). The key observation is that (4.1) can be viewed as a Galerkin discretization of (7.4). We then analyze the associated Galerkin scheme, prove its convergence, and derive an explicit convergence rate.

We begin by discretizing the underlying space K . Recall the level- m partition \mathcal{K}^m of K (cf. (4.4)). This partition induces a finite-dimensional subspace of $\mathcal{H} \doteq L^2(K, \nu)$, defined by

$$\mathcal{H}^m := \text{span}\{\mathbf{1}_A : A \in \mathcal{K}^m\}.$$

Throughout, $\mathbf{1}_A$ denotes the indicator function of the set A . Although the sets K_w and K_v corresponding to distinct $w, v \in \Sigma_m$ may intersect, their intersections have ν -measure zero by (3.14). Consequently, the resulting overlaps in the supports of the basis functions do not affect the convergence properties of the L^2 -projections onto \mathcal{H}^m .

We now construct the Galerkin approximation. The solution of the initial value problem (7.4)–(4.10) is approximated by a piecewise constant function of the form

$$u^m(t, x) = \sum_{|w|=m} u_w(t) \mathbf{1}_{K_w}(x). \quad (4.14)$$

Inserting (4.14) into (7.4) and projecting the resulting equation onto \mathcal{H}^m yields precisely the finite-dimensional system (4.1).

For later analysis, it is convenient to rewrite (4.1) as an evolution equation on \mathcal{H} :

$$\partial_t u^m(t, x) = f(u^m, t) + \int_K W^m(x, y) D(u^m(t, x), u^m(t, y)) d\nu(y), \quad (4.15)$$

where the discretized kernel W^m is given by

$$W^m := \sum_{|w|, |v|=m} W_{wv} \mathbf{1}_{K_w \times K_v}, \quad W_{wv} = \int_{K_w \times K_v} W d(\nu \times \nu). \quad (4.16)$$

The initial condition (4.10) is approximated in the same spirit by

$$g^m := \sum_{|w|=m} g_w \mathbf{1}_{K_w}, \quad g_w := \int_{K_w} g d\mu. \quad (4.17)$$

4.3 W-random self-similar networks and continuum limit

Along with the deterministic model (4.1), we consider an IPS on a random network:

$$\dot{u}_w = f(t, u_w) + \sum_{|v|=n} \xi_{wv} D(u_w, u_v) \nu(K_v), \quad w \in \Sigma_n, \quad (4.18)$$

where ξ_{wv} are independent Bernoulli random variables such that

$$\mathbb{P}(\xi_{wv} = 1) = \int_{G_{wv}} W d(\nu \times \nu), \quad \mathbb{P}(\xi_{wv} = 0) = 1 - \mathbb{P}(\xi_{wv} = 1). \quad (4.19)$$

For the random model, in addition to integrability of W we also assume $W \geq 0$ and $\int_{K \times K} W d(\nu \times \nu) = 1$.

In analogy to the graphon IPS, we expect that both the deterministic model (4.1) and its random counterpart (4.18) converge to the following nonlocal equation on K :

$$\partial_t u(t, x) = f(t, u) + \int_G W(x, y) D(u(t, x), u(t, y)) d\nu(y), \quad x \in K, \quad (4.20)$$

where ν is a stationary probability measure on K and $W \in L^1(K \times K, \nu \times \nu)$.

Likewise, if the IPS (4.1) is supplied with random initial conditions or has random parameters, we expect that in the large n limit its dynamics is captured by the Vlasov equation

$$\partial_t \bar{\rho}(t, u, x) + \partial_u \{V(t, u, x) \bar{\rho}(t, u, x)\} = 0, \quad (4.21)$$

$$V(t, x) = f(t, u) + \int_K \int_{R^k} W(x, y) D(u, v) \bar{\rho}(t, v, y) dv d\nu(y). \quad (4.22)$$

Here, $\bar{\rho}(t, \cdot, x)$ represents the probability density of the state of particle $x \in K$. Note that compared to (2.14), the label set K is fractal now and the the integral on the right-hand side of (4.22) is taken with respect to the stationary measure ν .

Our next goal is to justify (7.4) as the continuum limit of (4.1) and the Vlasov equation (4.21) as the mean-field limit of (4.18). The precise results are formulated in the two theorems below.

Theorem 4.3. *Let $u(t, x)$ be the solution of the IVP for (4.1) subject to $u(0, \cdot) = g \in L^2(K, \nu)$. Likewise, suppose*

$$u^n(t, x) = \sum_{|j|=n} u_j(t) \mathbf{1}_{K_j}(x),$$

$$\mathbf{u}^n(t, x) = \sum_{|j|=n} \mathbf{u}_j(t) \mathbf{1}_{K_j}(x),$$

solve the IVPs for (4.1) and (4.18), respectively, and satisfy

$$u_n(0, \cdot) = \mathbf{u}^n(0, \cdot) = g^n.$$

Then for $v \in \{u^n, \mathbf{u}^n\}$

$$\|u - v\|_{C(0, T; L^2(K, \nu))} \leq C (\|g - g^n\|_{L^2(K, \nu)} + \|W - W^n\|_{L^2(K \times K, \nu \times \nu)}). \quad (4.23)$$

Here, in case $v = \mathbf{u}^n$ estimate (4.23) holds almost surely, i.e., for almost every realization of the W -random graph (4.19).

Remark 4.4. *Estimate (4.23) can be extended to cover sparse self-similar networks in parallel to how this was done [67] for graphon IPS. Furthermore, the Large Deviation Principle from [35] translates to the self-similar setting as well.*

We next turn to the Vlasov equation on K . To this end, we adapt the definition of the local empirical measure to the present setting

$$\bar{\mathbf{m}}_{m, \ell, t}^x(A) = \frac{1}{\ell} \sum_{|j|=\ell} \mathbf{1}_A(u_{wj}(t)), \quad A \in \mathcal{B}(K), \quad x \in K_w, \quad |w| = m. \quad (4.24)$$

Further,

$$\bar{\mathbf{m}}_t^x(A) = \int_A \bar{\rho}(t, x, u) du, \quad A \in \mathcal{B}(K). \quad (4.25)$$

Thus, as in the case of graphon IPS we have

Theorem 4.5. *For given $\epsilon, T > 0$ and sufficiently large $m, \ell \in \mathbb{N}$, we have*

$$\sup_{t \in [0, T]} \int_K d_{BL}(\bar{\mathbf{m}}_{m, \ell, t}^x, \bar{\mathbf{m}}_t^x) d\nu(x) < \epsilon,$$

provided $\bar{\mathbf{m}}_{w, \ell, 0}^x$ converge weakly to $\bar{\mathbf{m}}_0^x$ for almost every $x \in K$ as $m, \ell \rightarrow \infty$.

We will address the question of the convergence rate for the discrete model (4.1) after proving Theorems 4.3 and 4.5.

5 Isomorphisms

In preparation for studying convergence of self-similar IPS, we establish an isomorphism between a given IFS $\mathcal{F} = \{f_i\}_{i \in [k]}$ with attractor K , equipped with a probability measure ν , and a canonical IFS $\mathcal{G} = \{g_i\}_{i \in [k]}$ whose attractor is the unit interval $Q = [0, 1]$, equipped with the Lebesgue measure λ . This isomorphism is then lifted, via pullbacks, to the function spaces $L^1(K, \nu)$ and $L^1(Q, \lambda)$, as well as to the corresponding product spaces $L^1(K \times K, \nu \times \nu)$ and $L^1(Q \times Q, \lambda \times \lambda)$. These identifications will be used in the next section to construct an isomorphism between self-similar IPS on K and their graphon counterparts on Q . In turn, this will allow us to translate existing convergence results for graphon IPS to their self-similar counterparts.

5.1 Auxiliary lemma

We begin with a technical lemma that will be used in what follows.

Let $\Sigma = [k]^{\mathbb{N}}$ be the symbolic space equipped with a Bernoulli probability measure μ . Consider the IFS $(L, \{f_i\}_{i \in [k]})$. Denote by $\pi_L : \Sigma \rightarrow L$ the natural projection and let $m = (\pi_L)_*\mu$. The triple $(L, \{f_i\}_{i \in [k]}, m)$ is referred to as a *probabilistic IFS*.

We consider the completions of μ and m and keep the same notation for the completed measures. Let \mathcal{A}_μ and \mathcal{A}_m denote the corresponding σ -algebras of measurable sets.

Assume that $(L, \{f_i\}_{i \in [k]}, m)$ satisfies the Lusin (N) property:

$$\mu(A) = 0 \implies m(\pi_L(A)) = 0 \quad \forall A \in \mathcal{A}_\mu. \quad (5.1)$$

Lemma 5.1. *Under the assumptions above, the following holds:*

1. $\pi_L(A) \in \mathcal{A}_m$ for every $A \in \mathcal{A}_\mu$.
2. $\pi_L^{-1}(A) \in \mathcal{A}_\mu$ for every $A \in \mathcal{A}_m$.
3. π_L is measure preserving, i.e.

$$m(A) = \mu(\pi_L^{-1}(A)) \quad \forall A \in \mathcal{A}_m.$$

Remark 5.2. Note that π maps null sets to null sets by the Lusin (N) property. Likewise, π^{-1} sends null sets to null sets by the definition of the pushforward measure $m = (\pi_L)_*\mu$.

Proof. 1. Let $A \in \mathcal{A}_\mu$. Since μ is the completion of a Borel measure on Σ , there exist a Borel set $B \subset \Sigma$ and a μ -null set N such that

$$A = B \cup N.$$

The map π_L is continuous, and Σ and L are Polish spaces; hence $\pi_L(B)$ is an analytic subset of L (cf. [55, Theorem 14.4]). Analytic sets are universally measurable (cf. [55, Theorem 21.10]) and, in particular, measurable with respect to any complete Borel measure, thus $\pi_L(B) \in \mathcal{A}_m$.

By the Lusin (N) property (5.1), $m(\pi_L(N)) = 0$, and since m is complete, $\pi_L(N) \in \mathcal{A}_m$. Therefore,

$$\pi_L(A) = \pi_L(B) \cup \pi_L(N) \in \mathcal{A}_m.$$

2. Let $A \in \mathcal{A}_m$. Since m is complete, there exist a Borel set $B \subset L$ and an m -null set N such that

$$A = B \cup N.$$

Because π_L is continuous, $\pi_L^{-1}(B)$ is a Borel subset of Σ , hence μ -measurable. Moreover,

$$\mu(\pi_L^{-1}(N)) = m(N) = 0.$$

Thus,

$$\pi_L^{-1}(A) = \pi_L^{-1}(B) \cup \pi_L^{-1}(N) \in \mathcal{A}_\mu.$$

3. The measure-preserving property follows directly from the definition of the pushforward measure $m = (\pi_L)_*\mu$: for every $A \in \mathcal{A}_m$,

$$m(A) = \mu(\pi_L^{-1}(A)).$$

□

5.2 Isomorphic IFSs

Let $K \subset \mathbb{R}^d$, the attractor of the contracting IFS $\{f_i\}_{i \in [k]}$, equipped with the self-similar measure $\nu_p = \pi_*\mu_p$ defined as the pushforward of the Bernoulli measure corresponding to the probability vector $p = (p_1, p_2, \dots, p_k)$ (cf. (3.12)). Without further mention, we assume that both the Bernoulli measure μ_p and its pushforward ν_p have been completed.

Denote by $\pi_K : \Sigma \rightarrow K$ the natural map. It is a continuous surjective map. However, it does not need to be injective. Denote the set on which the injectivity of π fails by

$$\mathcal{N}_{\pi_K} = \{w \in \Sigma : \text{card} \{\pi_K^{-1}(\pi_K(w))\} > 1\}. \quad (5.2)$$

We impose the following condition on (K, \mathcal{F}, ν_p) .

Assumption 5.3.

$$\mu_p(\mathcal{N}_{\pi_K}) = 0. \quad (5.3)$$

We illustrate Assumption 5.3 with the following examples.

Example 5.4. 1. The middle-third Cantor set, C , is the attractor of the IFS $\{f_1(x) = \frac{x}{3}, f_2(x) = \frac{x}{3} + \frac{2}{3}\}$. It satisfies the Strong Separation Condition: $f_1(C) \cap f_2(C) = \emptyset$. The natural projection π_C in this case is a bijection. Thus, $\mathcal{N}_{\pi_C} = \emptyset$ and $\mu_p(\mathcal{N}_{\pi_C}) = 0$.

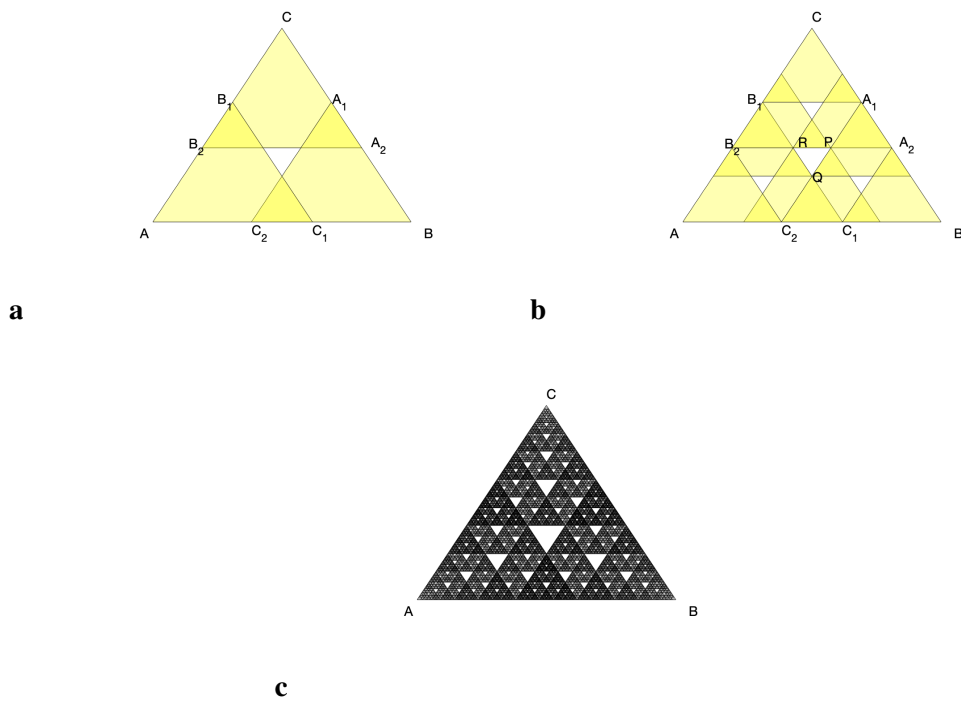


Figure 4: An example of a fat fractal. **a, b**) The first two steps of the construction of golden gasket. **c)** Approximation of the golden gasket.

2. *Sierpinski Gasket, G , is the attractor of a system of the three similitudes $\{f\}_{i \in [3]}$ (see (3.4)):*

$$G = \bigcup_{i=1}^3 f_i(G).$$

Unlike the Cantor set, SG does not satisfy the Strong Separation Condition, because there is an overlap between the images $f_1(G)$, $f_2(G)$, and $f_3(G)$:

$$f_i(G) \cap f_j(G) = f_i(v_j) = f_j(v_i), \quad i \neq j, \quad i, j \in [3].$$

The noninjectivity set \mathcal{N}_{π_G} is nonempty but it is countable and, thus, $\mu_p(\mathcal{N}_{\pi_G}) = 0$.

3. *Golden gasket Λ is the attractor of the following set of similitudes:*

$$f_i(x) = \lambda x + t_i, \quad i \in [3]; \quad t_1 = (0, 0), t_2 = (1 - \lambda, 0), t_3 = \left(\frac{1 - \lambda}{2}, \frac{\sqrt{3}(1 - \lambda)}{2} \right),$$

and $\lambda = \frac{\sqrt{5}-1}{2}$ is the reciprocal of the golden ratio (see Figure 4). This is an example of a fat gasket [12, 5].

By construction, $f_{122}(\Lambda) = f_{211}(\Lambda) = \Delta C_1 Q C_2$ (see Figure 4). Similarly, $f_{133}(\Lambda) = f_{311}(\Lambda)$ and $f_{233}(\Lambda) = f_{322}(\Lambda)$. Thus, all points in the cylinders $\Lambda_{122}, \Lambda_{133}, \Lambda_{233}$ have at least two different symbolic representations and, therefore, $\mu_p(\mathcal{N}_{\pi_\Lambda}) > 0$.

Given (K, \mathcal{F}, ν_p) , we will construct an isomorphic IFS $(Q, \mathcal{G}, \lambda_p)$ with $Q \doteq [0, 1]$. It will be used to establish connection between self-similar and graphon IPS.

We begin by specifying the type of the isomorphism between two probabilistic IPS which will be used below.

Definition 5.5. *Two probabilistic IFS $(A, \mathcal{F} = \{f_i\}_{i=1}^k, \nu)$ and $(\tilde{A}, \tilde{\mathcal{F}} = \{\tilde{f}_i\}_{i=1}^k, \tilde{\nu})$ are said to be isomorphic if there are subsets $A' \subset A$ and $\tilde{A}' \subset \tilde{A}$ of full measure and an invertible measure preserving map $\phi : \tilde{A}' \rightarrow A'$ such that*

$$\phi \circ f_i(x) = \tilde{f}_i \circ \phi(x) \quad \forall x \in A', \quad i \in [k]. \quad (5.4)$$

Consider the following IFS:

$$g_i(x) = \frac{x}{k} + x_{i-1}, \quad i \in [k], \quad (5.5)$$

where $x_i = \frac{i}{k}$, $i \in [k]$.

$Q = [0, 1]$ is the attractor of $\mathcal{G} = \{g_i\}_{i \in [k]}$

$$Q = \bigcup_{i=1}^k g_i(Q).$$

Define the natural projection $\pi_Q : \Sigma \rightarrow Q$:

$$\Sigma \ni w = (w_1 w_2 \dots) \mapsto \bigcap_{j=1}^{\infty} g_{w_1 w_2 \dots w_j}(Q). \quad (5.6)$$

Let $\lambda_p = (\pi_Q)_*\mu_p$ be the pushforward of the Bernoulli measure. On cylinders $Q_{w_1 w_2 \dots w_n} = g_{w_1 w_2 \dots w_n}(Q)$, we have

$$\lambda_p(Q_{w_1 w_2 \dots w_n}) = \mu_p(\pi_Q^{-1}(Q_{w_1 w_2 \dots w_n})) = p_{w_1} p_{w_2} \dots p_{w_n}. \quad (5.7)$$

In particular, for the uniform $p = (k^{-1}, k^{-1}, \dots, k^{-1})$, λ_p coincides with the Lebesgue measure.

Furthermore, λ_p is the unique stationary measure

$$\lambda_p(A) = \sum_{i=1}^k p_i \lambda_p(g_i^{-1}(A)) \quad \forall A \in \mathcal{B}(Q).$$

For $(Q, \mathcal{G}, \lambda_p)$, we verify the condition in Assumption 5.3.

Lemma 5.6.

$$\mu_p(\mathcal{N}_{\pi_Q}) = 0. \quad (5.8)$$

Proof. The noninjectivity set for π_Q is generated by the overlap set

$$\mathcal{O}(Q) = \bigcup_{1 \leq i < j \neq k} (g_i(Q) \cap g_j(Q)) = \left\{ \frac{1}{k}, \frac{2}{k}, \dots, \frac{k-1}{k} \right\}.$$

From this we define the critical set

$$\mathcal{C}(Q) = \pi_Q^{-1}(\mathcal{O}(Q)) = \{(1\dot{2}), (2\dot{1}), \dots, ((k-1)\dot{k}), (k(k-1))\},$$

where \dot{i} stands for $(ii \dots)$.

The noninjectivity set of π_Q is then given by

$$\mathcal{N}_{\pi_Q} = \bigcup_{w \in \Sigma^*} \bigcup_{\tau \in \mathcal{C}(Q)} (w\tau).$$

Since \mathcal{N}_{π_Q} is countable and μ_p is nonatomic, we have $\mu_p(\mathcal{N}_{\pi_Q}) = 0$. \square

Theorem 5.7. Suppose Assumption 5.3 holds. Then probabilistic IFS (K, \mathcal{F}, ν_p) and $(Q, \mathcal{G}, \lambda_p)$ are isomorphic.

Proof. 1. Assumption 5.3 implies that $(K, \{f_i\}_{i \in [k]}, \mu_p)$ satisfies the Lusin (N) property. Indeed, let $A \in \mathcal{A}_{\mu_p}$ with $\mu_p(A) = 0$. Since $\pi_K^{-1}(\pi_K(A)) = A \cup (\pi_K^{-1}(\pi_K(A)) \cap \mathcal{N}_{\pi_K})$ and $\mu_p(\mathcal{N}_{\pi_K}) = 0$, we obtain

$$\nu_p(\pi_K(A)) = \mu_p(\pi_K^{-1}(\pi_K(A))) = \mu_p(A) = 0.$$

Similarly, in view of Lemma 5.6, the system $(Q, \{g_i\}_{i \in [k]}, \nu_p)$ also satisfies the Lusin (N) property.

2. Define

$$\tilde{\Sigma} := \Sigma \setminus (\mathcal{N}_{\pi_K} \cup \mathcal{N}_{\pi_Q}), \quad \tilde{K} := \pi_K(\tilde{\Sigma}), \quad \tilde{Q} := \pi_Q(\tilde{\Sigma}).$$

By Assumption 5.3, Lemma 5.6, and Lemma 5.1,

$$\mu_p(\tilde{\Sigma}) = 1, \quad \nu_p(\tilde{K}) = 1, \quad \lambda_p(\tilde{Q}) = 1.$$

3. Let $\pi_{K1} := \pi_K|_{\tilde{\Sigma}}$ and $\pi_{Q1} := \pi_Q|_{\tilde{\Sigma}}$. Then both maps are bijections onto \tilde{K} and \tilde{Q} , respectively. Define

$$\beta := \pi_{K1} \circ \pi_{Q1}^{-1} : \tilde{Q} \rightarrow \tilde{K}.$$

Thus, β is a bijection between full-measure subsets of Q and K .

4. Since π_{K1} and π_{Q1} are measure-preserving bijections (cf. Lemma 5.1). The composition $\beta = \pi_{K1} \circ \pi_{Q1}^{-1}$ is measure-preserving as well.

5. Finally, using (3.9) and the fact that π_K and π_Q are injective when restricted to $\tilde{\Sigma}$, we derive

$$f_i \circ \beta = \beta \circ g_i, \quad g \in [k].$$

Therefore, (K, \mathcal{F}, ν_p) and $(Q, \mathcal{G}, \lambda_p)$ are isomorphic as probabilistic IFS. \square

We illustrate the construction of the isomorphism between two IFS in the proof of Theorem 5.7 with the following example.

Example 5.8. Consider SG , the attractor of the three similitudes

$$f_i(x) = \frac{1}{2}(x - v_i) + v_i, i \in [3]$$

(see Example 3.2). The overlap set for G

$$\mathcal{O}(G) = \{f_1(v_2) = f_2(v_1), f_1(v_3) = f_3(v_1), f_2(v_3) = f_3(v_2)\}.$$

The critical set

$$\mathcal{C}(G) = \pi_G^{-1}(\mathcal{O}(G)) = \{(1\dot{2}), (2\dot{1}), (3\dot{1}), (1\dot{3}), (2\dot{3}), (3\dot{2})\}.$$

The noninjectivity set of G

$$\mathcal{N}_{\pi_G} = \bigcup_{w \in \Sigma^*} \{(w1\dot{2}), (w2\dot{1}), (w3\dot{1}), (w1\dot{3}), (w2\dot{3}), (w3\dot{2})\}.$$

We equip K with the natural self-similar measure ν , i.e., $p = (\frac{1}{3}, \frac{1}{3}, \frac{1}{3})$. ν is proportional to $(\frac{\log 3}{\log 2})$ -dimensional Hausdorff measure (cf. Section 3.3).

The isomorphic IFS is then given by $(Q = [0, 1], \{g_i\}_{i \in [3]}, \lambda)$, where

$$g_i(x) = \frac{1}{3}(x - x_{i-1}) + x_{i-1}, \quad i \in [3],$$

with $x_j = \frac{j}{3}, j = 0, 1, 2, 3$. λ is the restriction of the Lebesgue measure to $[0, 1]$. The noninjectivity set of Q

$$\mathcal{N}_{\pi_Q} = \bigcup_{w \in \Sigma^*} \{(w1\dot{2}), (w2\dot{1}), (w2\dot{3}), (w3\dot{2})\}.$$

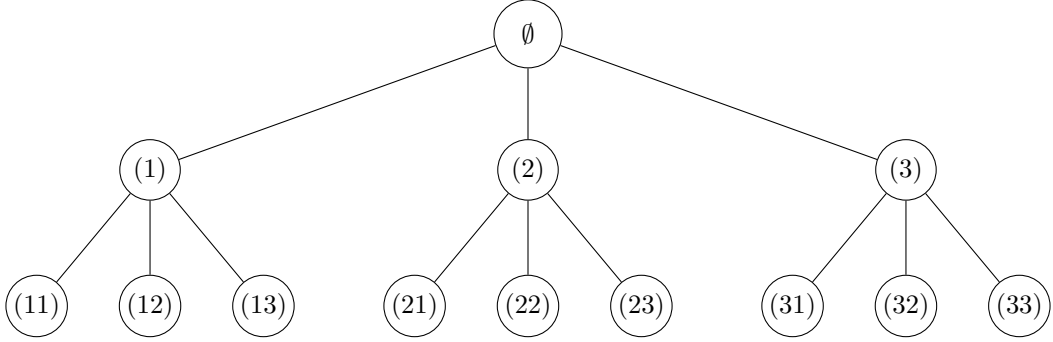


Figure 5: The root and first two levels of a tree representing SG.

It is instructive to represent the attractor of probabilistic IFS (G, \mathcal{F}, ν_p) with a rooted tree. The node set of the tree is given by the set of words from the alphabet $[k]$ of finite length, Σ^* (cf. 3.6). The adjacency is defined by the natural relation: $w \in \Sigma_n$ is a parent for all $(w_i) \in \Sigma_{n+1}$ with $i \in [k]$. The first two levels of the tree corresponding to the SG is illustrated in Fig. 5.

The isomorphic IFSs (G, \mathcal{F}, ν_p) and $(Q, \mathcal{G}, \lambda_p)$ share the same tree. Furthermore at each node $w \in \Sigma_n$, $\nu_p(K_w) = \lambda_p(Q_w) = \mu_p([w])$ (cf. (3.11)).

5.3 Isomorphic function spaces

Having constructed an isomorphic IFS $(Q, \mathcal{G}, \lambda_p)$, we now establish an isomorphism between $L^1(K, \nu_p)$ and $L^1(Q, \lambda_p)$. Since p is fixed, we henceforth omit it from the notation of the measures μ , ν , and λ .

In the remainder of this subsection, we focus on the relationship between $L^1(K, \nu)$ and $L^1(Q, \lambda)$. Throughout, it is understood that (K, \mathcal{F}, ν) and $(Q, \mathcal{G}, \lambda)$ are isomorphic probabilistic IFSs.

Recall that $\Sigma = [k]^{\mathbb{N}}$ is the symbolic space endowed with the Bernoulli measure μ .

Denote by

$$\pi_K : \Sigma \rightarrow K, \quad \pi_Q : \Sigma \rightarrow Q$$

the natural projections associated with the IFSs \mathcal{F} and \mathcal{G} , respectively.

By Assumption 5.3 and Lemma 5.6 the image measures

$$\nu = (\pi_K)_* \mu, \quad \lambda = (\pi_Q)_* \mu,$$

are measure-preserving.

We define the pullback operators

$$U_K : L^1(K, \nu) \rightarrow L^1(\Sigma, \mu), \quad U_Q : L^1(Q, \lambda) \rightarrow L^1(\Sigma, \mu),$$

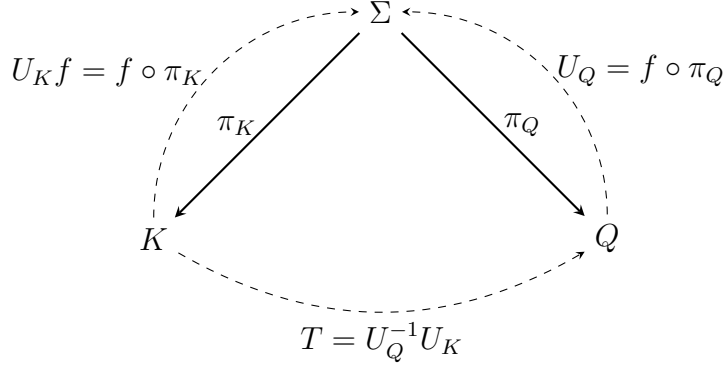


Figure 6: The isomorphism between measure spaces (K, ν) and (Q, λ) induces a corresponding isomorphism between the function spaces $L^1(K, \nu)$ and $L^1(Q, \lambda)$.

by

$$U_K f = f \circ \pi_K, \quad U_Q g = g \circ \pi_Q.$$

Since π_K and π_Q are measure-preserving, both operators are linear isometries onto their respective ranges. Here and throughout, the term *isometry* is understood in the L^1 -sense, namely as a linear map preserving the L^1 -norm. If one works in an L^2 setting instead, the isometries preserve the inner product as well.

Moreover, since π_Q is bijective μ -a.e., the inverse of U_Q is well-defined as an operator from $L^1(Q, \lambda)$ onto $L^1(\Sigma, \mu)$:

$$U_Q F = F \circ \pi_Q^{-1}. \quad (5.9)$$

This allows us to define a canonical operator

$$T : L^1(K, \nu) \longrightarrow L^1(Q, \lambda), \quad T f := U_Q^{-1}(U_K f), \quad (5.10)$$

Equivalently, $T f$ is the unique (up to λ -null sets) function satisfying

$$f \circ \pi_K = (T f) \circ \pi_Q \quad \mu\text{-a.e..} \quad (5.11)$$

By construction, T is a surjective linear isometry preserving positivity and integrals:

$$\int_K f d\nu = \int_Q T f d\lambda, \quad f \in L^1(K, \nu).$$

We emphasize that this identification is canonical up to null sets and depends only on the symbolic representation induced by the IFS. In particular, when the maps f_i are similitudes and ν is the natural self-similar measure, the operator T provides a concrete realization of functions on K as functions on the unit interval Q with respect to Lebesgue measure. This correspondence extends naturally to product spaces, yielding an isometric embedding of interaction kernels on $K \times K$ into the space of graphons $L^1(Q \times Q, \lambda \times \lambda)$.

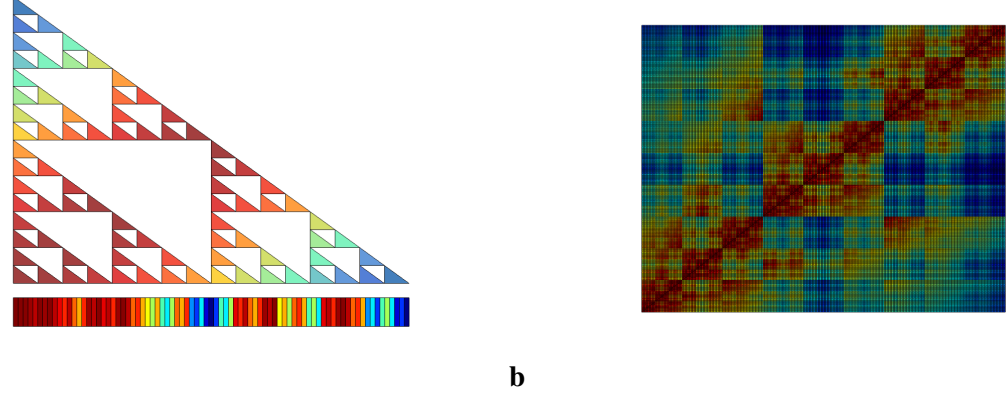


Figure 7: **a.** The heat map of the function $f(x) = e^{-|x_1 - x_2|}$ on $SG G \subset \mathbb{R}^2$ (above) and it is representation as a function on $[0, 1]$ (below). **b.** Graphon representation of $W(x, y) = e^{-\|x - y\|}$, $(x, y) \in G \times G \subset \mathbb{R}^2 \times \mathbb{R}^2$.

5.4 Martingale representation

In this subsection, we use martingales to compute $Tf \in L^1(Q, \lambda)$ for any given $f \in L^1(K, \nu)$ directly, without invoking symbolic space. Besides providing an alternative perspective on the isomorphism between $L^1(K, \nu)$ and $L^1(Q, \lambda)$, the martingale approach also yields a convenient method for the numerical approximation of Tf .

Given $f \in L^1(K, \mu)$, we generate a martingale sequence $(f_n, n \in \mathbb{N})$ as follows

$$f_n \doteq \mathbb{E}(f | \mathcal{K}_n)(x) = \sum_{w \in \Sigma_n} \nu_w(f) \mathbf{1}_{K_w}(x), \quad \nu_w(f) = \int_{K_w} f(y) d\nu(y),$$

where $\mathbb{E}(f | \mathcal{K}_n)$ stands for the conditional expectation with respect to the σ -algebra of subsets of $L^1(K, \nu)$, $\mathcal{K}_n = \sigma(\{K_w, w \in \Sigma_n\})$. By construction, $\mathbb{E}(f_{n+1} | \mathcal{K}_n) = f_n$. Thus, (f_n) form a martingale sequence converging to f ν -a.e. and in $L^1(K, \nu)$ by the Marcinkiewicz Theorem [80, Theorem 7.1.3].

Next, define $\tilde{f}_n : Q \rightarrow \mathbb{R}$ as follows

$$\tilde{f}_n(x) = \sum_{w \in \Sigma_n} \nu_w(f) \mathbf{1}_{Q_w}(x).$$

Theorem 5.9. Sequence (\tilde{f}_n) converges to $\tilde{f} \in L^1(Q, \lambda)$ λ -a.e. and in $L^1(Q, \lambda)$. Moreover, $\tilde{f} = Tf$.

Proof. 1. Let us check that (\tilde{f}_n) is a martingale sequence in $L^1(Q, \lambda)$:

$$\mathbb{E}(\tilde{f}_{n+1} | \mathcal{Q}_n) = \tilde{f}_n, \tag{5.12}$$

where $\mathcal{Q}_n = \sigma(\{Q_w, w \in \Sigma_n\})$.

Note

$$\begin{aligned}\mathbb{E}(\tilde{f}_{n+1}|\mathcal{Q}_n)(x) &= \sum_{w \in \Sigma_n} \frac{1}{\lambda(Q_w)} \left\{ \sum_{s \in [k]} \frac{1}{\lambda(Q_{ws})} \int_{K_{ws}} f(y) d\nu(y) \int_Q \mathbf{1}_{Q_{ws}}(x) d\lambda(x) \right\} \mathbf{1}_{Q_w}(x) \\ &= \sum_{w \in \Sigma_n} \int_{K_w} f(y) d\nu(y) \mathbf{1}_{Q_w}(x) = \tilde{f}_n(x),\end{aligned}$$

where we used $\nu(K_w) = \lambda(Q_w) = \mu([w])$ for all $w \in \Sigma_n$ and $n \in \mathbb{N}$.

2. By construction,

$$\|\tilde{f}_n\|_{L^1(Q, \lambda)} = \|f_n\|_{L^1(K, \nu)} = \|E(f|\mathcal{K}_n)\|_{L^1(K, \nu)} \rightarrow \|f\|_{L^1(K, \nu)} \quad \text{as } n \rightarrow \infty.$$

Thus,

$$\lim_{n \rightarrow \infty} \|\tilde{f}_n\|_{L^1(Q, \lambda)} = \|f\|_{L^1(K, \nu)}. \quad (5.13)$$

By the Martingale Convergence Theorem, $\lim_{n \rightarrow \infty} \tilde{f}_n = \tilde{f} \in L^1(Q, \lambda)$ λ -a.e. (cf. [80, Theorem 7.2.6]).

3. We want to show that (\tilde{f}_n) converges to \tilde{f} in $L^1(Q, \lambda)$ as well. To this end, we note that T maps $\mathbf{1}_{K_w}$ to $\mathbf{1}_{Q_w}$ for any $w \in \Sigma_m$ and $m \in \mathbb{N}$. This follows from the definition of T (5.10) and (5.9):

$$T\mathbf{1}_{K_w} = \mathbf{1}_{K_w} \circ \pi_K \circ \pi_Q^{-1} = \mathbf{1}_{[w]} \circ \pi_Q^{-1} = \mathbf{1}_{Q_w}.$$

By linearity, we conclude that $Tf_n = \tilde{f}_n$ and by (5.11),

$$f_n \circ \pi_K = \tilde{f}_n \circ \pi_Q \quad \mu - \text{a.e.} \quad (5.14)$$

After passing to $n \rightarrow \infty$ in (5.14), we have $Tf = \tilde{f}$.

Since T is L^1 -isometry, $\|\tilde{f}\|_{L^1(Q, \lambda)} = \|f\|_{L^1(K, \nu)}$. This combined with (5.13) yields

$$\lim_{n \rightarrow \infty} \|\tilde{f}_n\|_{L^1(Q, \lambda)} = \|\tilde{f}\|_{L^1(Q, \lambda)}. \quad (5.15)$$

With (5.15), the Martingale Convergence Theorem (cf. [80, Theorem 7.2.6]) implies that (\tilde{f}_n) converges to \tilde{f} in $L^1(Q, \lambda)$. Moreover,

$$\tilde{f}_n = \mathbb{E}(\tilde{f}|\mathcal{Q}_n).$$

□

Under the isomorphism constructed above, f and \tilde{f} generate the same projections

$$\nu_w(f) = \lambda_w(\tilde{f}) \quad \forall w \in \Sigma^*.$$

The same construction applied to $W \in L^1(K \times K, \nu \times \nu)$ yields $\tilde{W} \in L^1(Q \times Q, \lambda \times \lambda)$ defined by the limit

$$\tilde{W} = \lim_{n \rightarrow \infty} \tilde{W}_n, \quad \text{where} \quad \tilde{W}_n(x, y) \doteq \sum_{w, v \in \Sigma_n} \left(\int_{Q_w \times Q_v} W d(\mu \times \mu) \right) \mathbf{1}_{Q_w \times Q_v}(x, y).$$

This establishes the isomorphism between $L^1(K \times K, \nu \times \nu)$ and $L^1(Q \times Q, \lambda \times \lambda)$.

6 Convergence of self-similar IPS

The goal of this section is to prove Theorems 4.3 and 4.5. To this end, we use the results of the previous section to construct a graphon IPS that is isomorphic to the self-similar IPS (4.1). We then use this isomorphism, together with existing results for graphon IPS [64, 67, 53], to justify the continuum limit (4.20) and the Vlasov equation (4.21).

Since relating self-similar IPSs to their graphon counterparts is our main objective, throughout the remainder of this paper we assume, without further comment, that

$$p = (k^{-1}, k^{-1}, \dots, k^{-1}).$$

When the maps f_i are similitudes, this choice yields the natural self-similar measure on K . On Q , it always results in the restriction of the Lebesgue measure, so that the space of graphons is naturally identified with a subset of $L^1(Q \times Q, \lambda \times \lambda)$.

6.1 Isomorphic IPS

We now return to the self-similar IPS (4.20) on fractal K . Recall that K is an attractor of a probabilistic IFS $(K, \{f_i\}_{i \in [k]}, \nu)$. Following the recipe of § 5.2, we construct an isomorphic ISF $(Q, \{g_i\}_{i \in [k]}, \lambda)$, with

$$\Phi : \tilde{Q} \rightarrow \tilde{K} \tag{6.1}$$

denoting the corresponding measure preserving transformation such that

$$\Phi \circ f_i(x) = g_i \circ \Phi(x) \quad \forall x \in \tilde{K}, i \in [m].$$

Here, as above \tilde{K} denotes a subset of K of full measure and $\tilde{Q} = \Phi^{-1}(\tilde{K})$.

Next, we construct a graphon IPS on the unit interval Q that is isomorphic to the self-similar IPS (4.20) on the fractal K . To this end, we define $\tilde{W} : Q \times Q \rightarrow \mathbb{R}$ and $\tilde{g} : Q \rightarrow \mathbb{R}$ as follows

$$\tilde{W}(x, y) = \begin{cases} W_{\Phi^{-1}}(x, y) \doteq W(\Phi^{-1}(x), \Phi^{-1}(y)), & (x, y) \in \tilde{Q} \times \tilde{Q}, \\ 0, & \text{otherwise,} \end{cases} \tag{6.2}$$

$$\tilde{g}(x) = \begin{cases} g_{\Phi^{-1}}(x) \doteq g(\Phi^{-1}(x)), & x \in \tilde{Q}, \\ 0, & \text{otherwise.} \end{cases} \tag{6.3}$$

With these definitions in place, we consider the following graphon IPS

$$\dot{\tilde{u}}_w = f(t, \tilde{u}_w) + \sum_{|v|=n} \tilde{W}_{wv} D(\tilde{u}_w, \tilde{u}_v) \lambda(Q_v), \quad w \in \Sigma_n, \tag{6.4}$$

$$\tilde{u}_w(0) = \tilde{g}_w, \quad w \in \Sigma_n, \tag{6.5}$$

where

$$\tilde{W}_{wv} \doteq \int_{Q_w \times Q_v} \tilde{W}(x, y) d(\lambda \times \lambda)(x, y), \quad \tilde{g}_w \doteq \int_{Q_w} \tilde{g}(x) d\lambda(x).$$

By construction,

$$\begin{aligned}
W_{wv} &= \frac{1}{\nu(K_w)\nu(K_v)} \int_{K_w \times K_v} W(x, y) d(\nu \times \nu)(x, y) = \frac{1}{\nu(K_w)\nu(K_v)} \int_{\tilde{K}_w \times \tilde{K}_v} W(x, y) d(\nu \times \nu)(x, y) \\
&= \frac{1}{\lambda(Q_w)\lambda(Q_v)} \int_{\tilde{Q}_w \times \tilde{Q}_v} W_{\Phi^{-1}}(x, y) d(\nu \times \nu)(x, y) = \frac{1}{\lambda(Q_w)\lambda(Q_v)} \int_{\tilde{Q}_w \times \tilde{Q}_v} \tilde{W}(x, y) d(\lambda \times \lambda)(x, y) \\
&= \tilde{W}_{wv}.
\end{aligned}$$

Likewise,

$$\begin{aligned}
g_w &= \frac{1}{\nu(K_w)} \int_{K_w} g(x) d\nu(x) = \frac{1}{\nu(K_w)} \int_{\tilde{K}_w} g(x) d\nu(x) \\
&= \frac{1}{\lambda(Q_w)} \int_{\tilde{Q}_w} g_{\Phi^{-1}}(x) d\lambda(x) = \frac{1}{\lambda(Q_w)} \int_{Q_w} \tilde{g}(x) d\lambda(x) \\
&= \tilde{g}_w.
\end{aligned}$$

Since $W_{wv} = \tilde{W}_{wv}$ and $g_w = \tilde{g}_w$, the self-similar network (4.1) coincides with the graphon IPS (6.4) corresponding to graphon $\tilde{W} \in L^2(Q \times Q, \lambda \times \lambda)$.

6.2 The proofs of Theorems 4.3 and 4.5

With the graphon IPS (6.4) at hand, the proofs of Theorems 4.3 and 4.5 follow from Theorem 2.7 and Theorem 2.9, respectively.

Specifically, the correspondence between the kernels and initial data (cf. (6.2) and (6.3)) of the self-similar IPS (7.4), (4.10) and graphon IPS (2.12) with $W := \tilde{W}$ and initial data \tilde{g} translates into the following relation between the solutions of the two IVPs:

$$u(t, x) = \begin{cases} \tilde{u}(t, \Phi^{-1}(x)), & x \in \tilde{K}, \\ 0, & x \in K \setminus \tilde{K}. \end{cases} \quad (6.6)$$

From this we have,

$$\begin{aligned}
\|u^n(t, \cdot) - u(t, \cdot)\|_{L^2(K, \nu)} &= \|\tilde{u}^n(t, \Phi^{-1}(\cdot)) - \tilde{u}(t, \Phi^{-1}(\cdot))\|_{L^2(K, \nu)} \\
&= \|\tilde{u}^n(t, \cdot) - \tilde{u}(t, \cdot)\|_{L^2(Q, \lambda)} \rightarrow 0,
\end{aligned}$$

where we used Theorem 2.7 in the last step. This proves Theorem 4.3.

We proceed similarly to establish the relation between the empirical measures $\bar{m}_{m,\ell,t}^x$ and \bar{m}_t^x generated by the evolution of the self-similar IPS (4.1), (4.2) and its mean-field limit (4.21) on one hand and those generated by the graphon IPS (2.12) with $W := \tilde{W}$ and initial data \tilde{g} and the corresponding continuum limit (2.14). The latter are denoted by $m_{m,\ell,t}^x$ and m_t^x respectively. Recall that

$$m_t^x(B) = \int_B \rho(t, x, u) du,$$

where ρ satisfies the Vlasov equation (2.14) with $W := \tilde{W}$.

Using (6.1), we relate

$$\bar{\mathfrak{m}}_{m,\ell,t}^x(B) = \mathfrak{m}_{m,\ell,t}^{\Phi^{-1}(x)}(B) \quad \text{and} \quad \bar{\mathfrak{m}}_t^x(B) = \mathfrak{m}_t^{\Phi^{-1}(x)}(B) \quad \forall m, l \in \mathbb{Z} \quad t \in \mathbb{R}^+$$

for any Borel set B and $x \in \tilde{K}$. From this, it follows

$$\begin{aligned} \int_K d_{BL}(\bar{\mathfrak{m}}_{m,\ell,t}^x, \bar{\mathfrak{m}}_t^x) d\nu(x) &= \int_{\tilde{K}} d_{BL}(\bar{\mathfrak{m}}_{m,\ell,t}^x, \bar{\mathfrak{m}}_t^x) d\nu(x) \\ &= \int_{\tilde{K}} d_{BL}(\mathfrak{m}_{m,\ell,t}^{\Phi^{-1}(x)}, \mathfrak{m}_t^{\Phi^{-1}(x)}) d\nu(x) \\ &= \int_Q d_{BL}(\mathfrak{m}_{m,\ell,t}^y, \mathfrak{m}_t^y) d\lambda(y). \end{aligned}$$

By Theorem 2.9, $\sup_{t \in [0,T]} \int_Q d_{BL}(\mathfrak{m}_{m,\ell,t}^y, \mathfrak{m}_t^y) d\lambda(y)$ can be made less than any given $\epsilon > 0$ provided m and ℓ are large enough. This proves Theorem 4.5.

7 The rate of convergence

In this section, we develop a method for estimating the rate of convergence of the discrete models (4.1) and (4.2) on self-similar networks. By Theorem 4.3, the problem reduces to estimating the accuracy with which the graphon $W \in L^2(K \times K, \nu \times \nu)$ and the initial data $g \in L^2(K, \nu)$ are approximated by their L^2 -projections onto finite-dimensional subspaces of step functions on $K \times K$ and K , respectively:

$$\|W - W^n\|_{L^2(K \times K, \nu \times \nu)}, \quad \|g - g^n\|_{L^2(K, \nu)}.$$

The isomorphism between self-similar IPS and its graphon counterpart that was used to establish convergence of the discrete problems does not allow one to translate the information about convergence rates from graphon systems to self-similar networks. Therefore, in this section, we study the rate of convergence for the latter class of models directly.

For $\phi \in L^p(Q)$, a function on a Euclidean domain, the error of approximation by the L^2 -projection onto the subspace of step functions is determined by the L^p -Lipschitz regularity of $\phi \in \text{Lip}(\alpha, L^p(Q))$, $p \geq 1$, $0 < \alpha \leq 1$ (cf. Lemma 2.11). In the remainder of this section, we extend the definition of the generalized Lipschitz spaces to self-similar domains and use them to estimate the convergence rate for self-similar IPS.

Throughout this section, we assume that K is the attractor of the self-affine IFS (3.3), i.e., $f_i : \mathbb{R}^d \rightarrow \mathbb{R}^d$, $i \in [d]$, are contracting similitudes with the same contraction constant

$$|f_i(x) - f_i(y)| = \lambda |x - y|, \quad 0 < \lambda < 1, \quad x, y \in \mathbb{R}^d. \quad (7.1)$$

Further, let ν be the natural self-similar measure on K , i.e., $p_1 = p_2 = \dots = p_k = k^{-1}$ in (3.14).

Generalized Lipschitz spaces were key to estimating the rate of convergence for graphon IPSs (see Theorem 2.13). Naturally, we want to extend these spaces to fractal domains. The first step is to identify an appropriate analog of the modulus of continuity in the fractal setting.

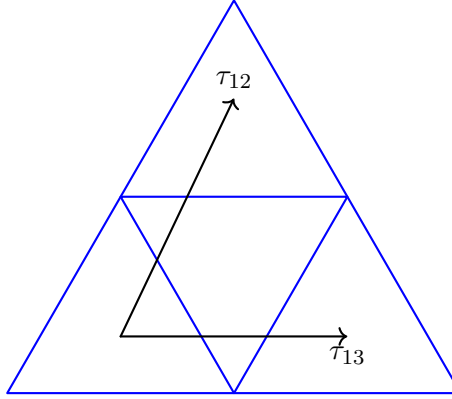


Figure 8: Vectors τ_{12} and τ_{13} , which are used in the definition of the modulus of continuity (see Definition 7.1) when applied to functions on SG.

For a Euclidean domain Q , the modulus of continuity measures the difference between $f \in L^p(Q)$ and its translation $f(\cdot + h)$ for small $|h|$ (cf. (2.22)). When attempting to extend this notion to the fractal setting, we immediately encounter the following difficulty: given $x \in K$ and $h \in \mathbb{R}^d$, the point $x + h$ need not belong to K , even for arbitrarily small $|h|$. Consequently, the first step is to identify an appropriate analog of translation on K .

To this end, for $i, j \in [k]$, $i \neq j$, we define τ_{ij} to be the unique vector such that

$$f_j(K) = f_i(K) + \tau_{ij}. \quad (7.2)$$

See Figure 8 for an illustration of the vectors τ_{ij} for SG.

With (τ_{ij}) in hand, we are now prepared to define the modulus of continuity at level $m \in \mathbb{N}$.

Definition 7.1. For $\phi \in L^p(K, \nu)$, define the L^p -modulus of continuity at level $m \in \mathbb{N}$ as follows

$$\omega_p(\phi, m) = \sup_{\ell \geq m} \max_{i \neq j} \left\{ \|\phi(\cdot + \tau) - \phi(\cdot)\|_{L^p(\tilde{K}_\tau, \mu)} : \tau = \lambda^{-(\ell+1)} \tau_{ij}, i, j \in S \right\},$$

where

$$\tilde{K}_\tau = \{x \in K : x + \tau \in K\}.$$

The generalized Lipschitz spaces are now defined in direct analogy to the Euclidean case.

Definition 7.2. For $\alpha \in (0, 1]$, define the generalized Lipschitz space

$$\text{Lip}(\alpha, L^p(K, \nu)) = \{\phi \in L^p(K, \nu) : \exists C > 0 \text{ such that } \omega_p(\phi, m) \leq C \lambda^{\alpha m}\},$$

equipped with the norm

$$\|\phi\|_{\text{Lip}(\alpha, L^p(K, \nu))} \doteq \sup_{m \in \mathbb{N}} \lambda^{-\alpha m} \omega_p(\phi, m).$$

Remark 7.3. This definition provides a natural generalization of Nikolskii–Besov spaces to the fractal setting (cf. [9]).

The following lemma yields the error of approximation of an L^p -function on K by L^2 -projection onto a finite-dimensional subspace of functions that are constant on m -cylinders of K .

Lemma 7.4. Let $\{f_i\}_{i \in [k]}$ be a system on contracting similitudes with attractor K equipped with natural self-similar measure ν satisfying (3.14) and consider $\phi \in \text{Lip}(\alpha, L^p(K, \nu))$. Then

$$\|\phi^m - \phi\|_{L^p(K, \nu)} \leq \frac{k^{1/p-1} (k-1)^{1/p}}{1 - \lambda^\alpha} \|\phi\|_{\text{Lip}(L^p(K, \nu))} \lambda^{\alpha m}. \quad (7.3)$$

Remark 7.5. To apply Lemma 7.4 to $W \in \text{Lip}(\alpha, L^2(K \times K, \nu \times \nu))$, we note that $K \times K$ is the attractor of similitudes $\{f_{ij} = (f_i, f_j)\}_{i,j \in [k]}$ with the same contraction constant λ . Therefore, (7.3) applies to $W \in L^p(K \times K, \nu \times \nu)$ after replacing k by k^2 .

The combination of Lemma 7.4 and Theorem 4.3 yields the following theorem.

Theorem 7.6. Let $u(t, x)$ be the solution of the IVP for (4.1) subject to $u(0, \cdot) = g \in \text{Lip}(\alpha_1, L^2(K, \nu))$. Suppose further that $W \in \text{Lip}(\alpha_2, L^2(K \times K, \nu \times \nu))$. The solutions of the discrete problems u^n and u^n , as described in Theorem 4.3, and $v \in \{u^n, u^n\}$. Then

$$\|u - v\|_{C(0, T; L^2(K, \nu))} \leq C \lambda^{-\alpha m}, \quad \alpha = \min\{\alpha_1, \alpha_2\}. \quad (7.4)$$

Here, in case $v = u^n$ estimate (4.23) holds almost surely.

It remains to prove Lemma 7.4.

Proof of Lemma 7.4. Fix $m \geq 1$ and partition K into k^m subsets

$$K_w = f_w(K), \quad w \in \Sigma_m.$$

We represent ϕ^{m+1} as

$$\phi^{m+1} = \sum_{|w|=m} \sum_{j \in I} \phi_{w,j} \mathbf{1}_{K_{wj}}, \quad (7.5)$$

where

$$\phi_{wj} = \int_{K_{wj}} \phi d\nu.$$

Likewise,

$$\begin{aligned} \phi^m &= \sum_{|w|=m} \sum_{j \in [k]} \phi_w \mathbf{1}_{K_{wj}} \\ &= d^{-1} \sum_{|w|=m} \sum_{j \in [k]} \sum_{l \in [k]} \phi_{wl} \mathbf{1}_{K_{wj}}, \end{aligned} \quad (7.6)$$

where we used $\nu(K_{wj}) = k^{-1}\nu(K_w)$, which follows from the fact that ν satisfies (cf. 3.14) with $p_i = k^{-1}, i \in [k]$.

By subtracting (7.5) from (7.6), we have

$$\begin{aligned} k(\phi^m(x) - \phi^{m+1}(x)) &= \sum_{|w|=m, j \in [k]} \sum_{l \neq j} \left(\int_{K_{wj}} - \int_{K_{wl}} \right) \phi(z) dz \mathbf{1}_{K_{wj}}(x) \\ &= \sum_{|w|=m} \sum_{j \in [k]} \sum_{l \neq j} \int_{K_{wj}} [\phi(y + \tau_{jl}^m) - \phi(y)] d\nu(y) \mathbf{1}_{K_{wj}}(x), \end{aligned} \quad (7.7)$$

where

$$\tau_{ij}^m = \lambda^m \tau_{ij}, \quad i, j \in [k], i \neq j.$$

After raising both sides of (7.7) to the p th power and integrating over K , we have

$$\begin{aligned} k^p \int |\phi^m - \phi^{m+1}|^p d\mu &= \sum_{w,j,l} \left| \int_{K_{wj}} [\phi(y + \tau_{jk}^m) - \phi(y)] d\nu(y) \right|^p \nu(K_{wj}) \\ &\leq \sum_{j,l \in [k]} \sum_w \int_{K_{wj}} |\phi(y + \tau_{jl}^m) - \phi(y)|^p d\mu(y) \\ &\leq k(k-1)\omega_p^p(\phi, m). \end{aligned}$$

From this we conclude

$$\|\phi^m - \phi^{m+1}\|_{L^p(K, \mu)} \leq \frac{(d(d-1))^{1/p}}{d} \omega_p(\phi, m).$$

For any integer $M > m$ we have

$$\begin{aligned} \|\phi^m - \phi^{m+M}\|_{L^p(K, \nu)} &\leq \sum_{k=m}^{\infty} \|\phi^k - \phi^{k+1}\|_{L^p(K, \nu)} \\ &\leq \frac{(k(k-1))^{1/p}}{k} \|\phi\|_{\text{Lip}(L^p(K, \nu))} \frac{\lambda^{\alpha m}}{1 - \lambda^\alpha}. \end{aligned} \quad (7.8)$$

By passing M to infinity in (7.8), we get (7.3). □

8 Discussion

The results of this work establish a unified framework for studying IPSs on self-similar networks and for understanding their macroscopic behavior through continuum and mean-field limits posed on fractal domains. Our analysis shows that the large-scale dynamics of IPS defined on self-similar networks admit limiting descriptions that are exactly the same as in the graphon setting. In particular, we demonstrate an

explicit isomorphism between self-similar IPS and their graphon counterparts. This correspondence can be effectively used to justify the Vlasov equation as the mean-field limit for self-similar IPS.

Another important contribution of this work is rate of convergence convergence estimates for discrete self-similar models. In contrast to the Euclidean case, where one can use generalized Lipschitz spaces, which are well-known in analysis, the construction of the function spaces in the fractal setting requires careful adaptation of generalized Lipschitz spaces to functions on fractal domains. The scale of generalized Lipschitz spaces introduced in this paper, together with the corresponding estimates for L^2 -projections onto piecewise constant subspaces, provides foundation for the rate of convergence analysis of the Galerkin method for models on fractal domains. We show that these spaces afford the minimal regularity required to obtain sharp convergence rates for the discontinuous Galerkin approximations of nonlocal equations on fractal sets.

Modeling of many physical, biological, and technological systems involve geometric structures that are not well approximated by Euclidean domains. Hierarchical networks, porous media, and biological tissue frequently exhibit self-similarity at multiple scales. The approach developed in this paper suggests a new class of PDE models on fractals, models that may help to better understand transport and diffusion in heterogeneous media on the one hand, and synchronization and collective dynamics in self-similar networks on the other.

Several promising directions stem naturally from the present work. One is the extension of the theory to IPS with stochastic forcing similar to how it was done for graphon IPS in [71], another is the exploration of nonlocal diffusion on fractal sets. Further, the results of this work open a way for studying transition to synchronization in the Kuramoto model on self-similar networks along the lines of the analysis of the Kuramoto model on graphs [24, 25]. It is also of interest to explore whether the isomorphism between graphon and self-similar IPS extends to models on other spaces with partitions [57]. Finally, given the growing interest in data and machine-learning, the techniques developed in this paper may find applications in the analysis of complex networks inferred from data and networks used in training large language models [81].

Acknowledgements. This work was partially supported by NSF grant DMS 2406941.

A Integration of functions on self-similar domains

The implementation of the Galerkin scheme on self-similar domains as described in § 4.2 requires evaluation of the integrals of the form

$$\int_{K_w \times K_v} W d(\mu \times \mu) \quad \text{and} \quad \int_{K_w} g d\mu \quad w, v \in \Sigma_m.$$

By reasons explained in Remark 7.5, it is sufficient to address this problem for $\int_{K_w} \phi d\mu$ with $\phi \in L^1(K, \mu)$. Furthermore, since

$$\frac{\mu(\cdot)}{\mu(K_w)}$$

is a probability measure on K_w , without loss of generality we may consider

$$\int_K \phi d\nu, \quad \phi \in L^1(\phi, \nu). \quad (\text{A.1})$$

Therefore, in the remainder of this section we will focus on the problem of evaluation of (A.1).

Throughout this section, K is an attractor of a system of contracting similitudes $\{f_i\}_{i \in [k]}$ equipped with the natural self-similar probability measure ν , i.e., $(K, \{f_i\}_{i \in [k]}, \nu)$ is a probabilistic IFS. Further, we assume (5.3), which in turn implies (3.14).

A.1 Monte-Carlo method

Bernoulli measure μ is an ergodic probability measure invariant under σ and by the Ergodic Theorem (cf. [37, Theorem 6.1]), for μ -a.e. $x \in \Sigma$, we have

$$\begin{aligned} \lim_{m \rightarrow \infty} \frac{1}{m} \sum_{j=1}^{m-1} \phi(\pi(\sigma^j(x))) &= \int_{\Sigma} \phi \circ \pi(x) d\mu(x) \\ &= \int_K \phi(y) d\nu(y), \end{aligned} \quad (\text{A.2})$$

where we used $\nu = \pi_* \mu$ in the second line.

To approximate $\int_K \phi d\nu$ we choose a random $x \in \Sigma$ as follows:

$$x = (x_1, x_2, \dots, x_{2M}, \dots), \quad (x_1, x_2, \dots, x_{2M}) \sim \text{Uniform}(\Sigma_{2M}), M \gg 1.$$

Then

$$\frac{1}{M} \sum_{j=0}^{M-1} \phi(\pi \circ \sigma^j(x)) = \frac{1}{M} \sum_{j=0}^{M-1} \phi(\pi(\xi_j)),$$

where

$$\xi_j := \sigma^j(x) = (x_{1+j}, x_{2+j}, \dots) \in \Sigma.$$

Finally, we approximate

$$\phi(\pi(\xi_j)) \approx \frac{1}{k} \sum_{i=1}^k \phi(\pi(x_{1+j}, x_{2+j}, \dots, x_{M+j}, i)), \quad j = 0, 1, 2, \dots, M-1.$$

Thus,

$$\frac{1}{M} \sum_{j=0}^{M-1} \phi(\pi \circ \sigma^j(x)) \approx \frac{1}{Mk} \sum_{j=0}^{M-1} \sum_{i=1}^k \phi(\pi(x_{1+j}, x_{2+j}, \dots, x_{M+j}, i)) =: S_M.$$

For large M , S_M approximates $\int_K \phi d\nu$.

A.2 Quasi-Monte-Carlo method

A similar algorithm can be developed using uniform sequences (cf. [48]).

To this end, pick $x_0 \in K$ and compute

$$x_w = f_w(x_0), \quad w \in \Sigma_m.$$

By Theorem 3.1 in [48], $\{x_w\}_{w \in \Sigma_m}$ is a uniform sequence. Consequently for $\phi \in C(K)$, we have

$$\lim_{m \rightarrow \infty} \left| \frac{1}{m^k} \sum_{|w|=m} \phi(x_w) - \int_K \phi d\nu \right| = 0. \quad (\text{A.3})$$

We expect that the rate of convergence in (A.3) is of order m^{-k} due to Koksma-Hlawka inequality available in closely related setting (cf. [48]). However, we are not aware of the proof of this inequality for the problem at hand.

References

- [1] Manuela Aguiar, Christian Bick, and Ana Dias, *Network dynamics with higher-order interactions: coupled cell hypernetworks for identical cells and synchrony*, Nonlinearity **36** (2023), no. 9, 4641–4673 (English).
- [2] Artem Alexandrov and Georgi S. Medvedev, *Phase transitions in the Ising model on random graphs*, Preprint, arXiv:2511.10838 [math-ph] (2025), 2025.
- [3] Alexander Aurell, René Carmona, Gökçe Dayanıklı, and Mathieu Laurière, *Finite state graphon games with applications to epidemics*, Dyn. Games Appl. **12** (2022), no. 1, 49–81 (English).
- [4] Blanca Ayuso de Dios, Simone Dovetta, and Laura V. Spinolo, *On the continuum limit of epidemiological models on graphs: convergence and approximation results*, Math. Models Methods Appl. Sci. **34** (2024), no. 8, 1483–1532 (English).
- [5] Balázs Bárány, Károly Simon, and Boris Solomyak, *Self-similar and self-affine sets and measures*, Math. Surv. Monogr., vol. 276, Providence, RI: American Mathematical Society (AMS), 2023 (English).
- [6] Daniel ben Avraham and Shlomo Havlin, *Diffusion and reactions in fractals and disordered systems*, Cambridge: Cambridge University Press, 2000 (English).
- [7] Gianmarco Bet, Fabio Coppini, and Francesca Romana Nardi, *Weakly interacting oscillators on dense random graphs*, J. Appl. Probab. **61** (2024), no. 1, 255–278 (English).
- [8] Christopher J. Bishop and Yuval Peres, *Fractals in probability and analysis*, Camb. Stud. Adv. Math., vol. 162, Cambridge: Cambridge University Press, 2017 (English).

- [9] Vladimir I. Bogachev, Egor D. Kosov, and Svetlana N. Popova, *A new approach to Nikolskii-Besov classes*, Mosc. Math. J. **19** (2019), no. 4, 619–654 (English).
- [10] Christian Borgs, Jennifer T. Chayes, Henry Cohn, and Yufei Zhao, *An L^p theory of sparse graph convergence I: Limits, sparse random graph models, and power law distributions*, Trans. Amer. Math. Soc. **372** (2019), no. 5, 3019–3062. MR 3988601
- [11] Lucas Böttcher and Mason A. Porter, *Dynamical processes on metric networks*, SIAM J. Appl. Dyn. Syst. **24** (2025), no. 4, 2848–2885 (English).
- [12] Dave Broomhead, James Montaldi, and Nikita Sidorov, *Golden gaskets: variations on the Sierpiński sieve*, Nonlinearity **17** (2004), no. 4, 1455–1480 (English).
- [13] Armin Bunde and Shlomo Havlin (eds.), *Fractals and disordered systems.*, 2nd rev. and enlarged ed. ed., Berlin: Springer-Verlag, 1996 (English).
- [14] A. M. Caetano, S. N. Chandler-Wilde, X. Claeys, A. Gibbs, D. P. Hewett, and A. Moiola, *Integral equation methods for acoustic scattering by fractals*, Preprint, arXiv:2309.02184 [math.NA] (2023), 2023.
- [15] ———, *Integral equation methods for acoustic scattering by fractals*, Preprint, arXiv:2309.02184 [math.NA] (2023), 2023.
- [16] A. M. Caetano, S. N. Chandler-Wilde, A. Gibbs, D. P. Hewett, and A. Moiola, *A Hausdorff-measure boundary element method for acoustic scattering by fractal screens*, Numer. Math. **156** (2024), no. 2, 463–532 (English).
- [17] Peter E. Caines and Minyi Huang, *Graphon mean field games and their equations*, SIAM J. Control Optim. **59** (2021), no. 6, 4373–4399. MR 4340663
- [18] Sourav Chatterjee, *Large deviations for random graphs*, Lecture Notes in Mathematics, vol. 2197, Springer, Cham, 2017, Lecture notes from the 45th Probability Summer School held in Saint-Flour, June 2015, École d’Été de Probabilités de Saint-Flour. [Saint-Flour Probability Summer School]. MR 3700183
- [19] Hayato Chiba and Georgi S. Medvedev, *The mean field analysis of the Kuramoto model on graphs I. The mean field equation and transition point formulas*, Discrete Contin. Dyn. Syst. **39** (2019), no. 1, 131–155. MR 3918168
- [20] ———, *The mean field analysis of the Kuramoto model on graphs II. Asymptotic stability of the incoherent state, center manifold reduction, and bifurcations*, Discrete Contin. Dyn. Syst. **39** (2019), no. 7, 3897–3921. MR 3960490
- [21] ———, *Stability and bifurcation of mixing in the Kuramoto model with inertia*, SIAM J. Math. Anal. **54** (2022), no. 2, 1797–1819. MR 4396969
- [22] Hayato Chiba, Georgi S. Medvedev, and Matthew S. Mizuhara, *Bifurcations in the Kuramoto model on graphs*, Chaos **28** (2018), no. 7, 073109, 10. MR 3833337
- [23] ———, *Bifurcations in the Kuramoto model on graphs*, Chaos **28** (2018), no. 7, 073109, 10 (English).

- [24] ———, *Instability of mixing in the Kuramoto model: From bifurcations to patterns*, Pure and Applied Functional Analysis **7** (2022), 1159–1172.
- [25] ———, *Bifurcations and patterns in the Kuramoto model with inertia*, J. Nonlinear Sci. **33** (2023), no. 5, 21 (English), Id/No 78.
- [26] Fabio Coppini, *Long time dynamics for interacting oscillators on graphs*, Ann. Appl. Probab. **32** (2022), no. 1, 360–391 (English).
- [27] ———, *A note on Fokker-Planck equations and graphons*, J. Stat. Phys. **187** (2022), no. 2, 12 (English), Id/No 15.
- [28] Clément Cosco and Assaf Shapira, *Topologically induced metastability in a periodic XY chain*, J. Math. Phys. **62** (2021), no. 4, 15 (English), Id/No 043301.
- [29] Felipe Cucker and Steve Smale, *Emergent behavior in flocks*, IEEE Trans. Autom. Control **52** (2007), no. 5, 852–862 (English).
- [30] Yu. L. Daletskij and M. G. Krejn, *Stability of solutions of differential equations in Banach space. Translated from the Russian by S. Smith*, Transl. Math. Monogr., vol. 43, American Mathematical Society (AMS), Providence, RI, 1974 (English).
- [31] Ronald A. DeVore and George G. Lorentz, *Constructive approximation*, Grundlehren der Mathematischen Wissenschaften [Fundamental Principles of Mathematical Sciences], vol. 303, Springer-Verlag, Berlin, 1993. MR 1261635
- [32] R. L. Dobrushin, *Vlasov equations*, Funct. Anal. Appl. **13** (1979), 115–123 (English).
- [33] Florian Dörfler and Francesco Bullo, *Synchronization and transient stability in power networks and nonuniform Kuramoto oscillators*, SIAM J. Control Optim. **50** (2012), no. 3, 1616–1642 (English).
- [34] R. M. Dudley, *Real analysis and probability*, Cambridge Studies in Advanced Mathematics, vol. 74, Cambridge University Press, Cambridge, 2002, Revised reprint of the 1989 original. MR 1932358
- [35] Paul Dupuis and Georgi S. Medvedev, *The large deviation principle for interacting dynamical systems on random graphs*, Comm. Math. Phys. **390** (2022), no. 2, 545–575. MR 4384715
- [36] K. J. Falconer, *Semilinear PDEs on self-similar fractals*, Commun. Math. Phys. **206** (1999), no. 1, 235–245 (English).
- [37] Kenneth Falconer, *Techniques in fractal geometry*, John Wiley & Sons, Ltd., Chichester, 1997. MR 1449135
- [38] ———, *Fractal geometry*, third ed., John Wiley & Sons, Ltd., Chichester, 2014, Mathematical foundations and applications. MR 3236784
- [39] Kenneth J. Falconer and Jiaxin Hu, *Nonlinear diffusion equations on unbounded fractal domains*, J. Math. Anal. Appl. **256** (2001), no. 2, 606–624 (English).
- [40] Shuang Gao and Peter E. Caines, *Graphon control of large-scale networks of linear systems*, IEEE Trans. Automat. Control **65** (2020), no. 10, 4090–4105. MR 4159107

- [41] Marios Antonios Gkogkas, Benjamin Jüttner, Christian Kuehn, and Erik Andreas Martens, *Graphop mean-field limits and synchronization for the stochastic Kuramoto model*, Chaos **32** (2022), no. 11, 13 (English), Id/No 113120.
- [42] Marios Antonios Gkogkas and Christian Kuehn, *Graphop mean-field limits for Kuramoto-type models*, SIAM J. Appl. Dyn. Syst. **21** (2022), no. 1, 248–283 (English).
- [43] François Golse, *On the dynamics of large particle systems in the mean field limit*, Macroscopic and large scale phenomena: coarse graining, mean field limits and ergodicity, Lect. Notes Appl. Math. Mech., vol. 3, Springer, [Cham], 2016, pp. 1–144. MR 3468297
- [44] Yosra Hafiene, Jalal M. Fadili, Christophe Chesneau, and Abderrahim Elmoataz, *Continuum limit of the nonlocal p -Laplacian evolution problem on random inhomogeneous graphs*, ESAIM, Math. Model. Numer. Anal. **54** (2020), no. 2, 565–589 (English).
- [45] Rainer Hegselmann and Ulrich Krause, *Opinion dynamics driven by various ways of averaging*, Comput. Econ. **25** (2005), no. 4, 381–405 (English).
- [46] Michael Hinz, Dorina Koch, and Melissa Meinert, *Sobolev spaces and calculus of variations on fractals*, Analysis, probability and mathematical physics on fractals. Based on the presentations at the 6th conference, Cornell University, Ithaca, NY, USA, June 2017, Hackensack, NJ: World Scientific, 2020, pp. 419–450 (English).
- [47] John E. Hutchinson, *Fractals and self-similarity*, Indiana Univ. Math. J. **30** (1981), no. 5, 713–747. MR 625600
- [48] Maria Infusino and Aljoša Volčič, *Uniform distribution on fractals*, Unif. Distrib. Theory **4** (2009), no. 2, 47–58. MR 2559412
- [49] Pierre-Emmanuel Jabin, *A review of the mean field limits for Vlasov equations*, Kinet. Relat. Models **7** (2014), no. 4, 661–711. MR 3317577
- [50] Pierre-Emmanuel Jabin and Datong Zhou, *The mean-field Limit of sparse networks of integrate and fire neurons*, Preprint, arXiv:2309.04046 [math.PR] (2023), 2023.
- [51] Anders Johansson, Anders Öberg, and Mark Pollicott, *Ergodic theory of Kusuoka measures*, J. Fractal Geom. **4** (2017), no. 2, 185–214 (English).
- [52] Dmitry Kaliuzhnyi-Verbovetskyi and Georgi S. Medvedev, *The semilinear heat equation on sparse random graphs*, SIAM J. Math. Anal. **49** (2017), no. 2, 1333–1355. MR 3634990
- [53] ———, *The Mean Field Equation for the Kuramoto Model on Graph Sequences with Non-Lipschitz Limit*, SIAM J. Math. Anal. **50** (2018), no. 3, 2441–2465. MR 3799057
- [54] ———, *Sparse Monte Carlo method for nonlocal diffusion problems*, SIAM J. Numer. Anal. **60** (2022), no. 6, 3001–3028. MR 4500528
- [55] Alexander S. Kechris, *Classical descriptive set theory*, Grad. Texts Math., vol. 156, Berlin: Springer-Verlag, 1995 (English).

- [56] Jun Kigami, *Analysis on fractals*, Cambridge Tracts in Mathematics, vol. 143, Cambridge University Press, Cambridge, 2001. MR 1840042
- [57] ———, *Geometry and analysis of metric spaces via weighted partitions*, Lect. Notes Math., vol. 2265, Cham: Springer, 2020 (English).
- [58] Christian Kuehn and Chuang Xu, *Vlasov equations on digraph measures*, J. Differ. Equations **339** (2022), 261–349 (English).
- [59] ———, *Vlasov equations on directed hypergraph measures*, SN Partial Differ. Equ. Appl. **6** (2025), no. 1, 49 (English), Id/No 9.
- [60] Y. Kuramoto, *Cooperative dynamics of oscillator community*, Progress of Theor. Physics Supplement (1984), 223–240.
- [61] Vito Latora, Andrea Rapisarda, and Stefano Ruffo, *Chaos and statistical mechanics in the Hamiltonian mean field model.*, Physica D **131** (1999), no. 1-4, 38–54 (English).
- [62] László Lovász, *Large networks and graph limits*, American Mathematical Society Colloquium Publications, vol. 60, American Mathematical Society, Providence, RI, 2012. MR 3012035
- [63] Eric Luçon, *Quenched asymptotics for interacting diffusions on inhomogeneous random graphs*, Stochastic Process. Appl. **130** (2020), no. 11, 6783–6842. MR 4158803
- [64] Georgi S. Medvedev, *The nonlinear heat equation on dense graphs and graph limits*, SIAM J. Math. Anal. **46** (2014), no. 4, 2743–2766. MR 3238494
- [65] ———, *The nonlinear heat equation on W -random graphs*, Arch. Ration. Mech. Anal. **212** (2014), no. 3, 781–803 (English).
- [66] ———, *Small-world networks of Kuramoto oscillators*, Phys. D **266** (2014), 13–22. MR 3129708
- [67] ———, *The continuum limit of the Kuramoto model on sparse random graphs*, Communications in Mathematical Sciences **17** (2019), no. 4, 883–898.
- [68] Georgi S. Medvedev and Matthew S. Mizuhara, *Chimeras unfolded*, J. Stat. Phys. **186** (2022), no. 3, Paper No. 46, 19. MR 4381194
- [69] Georgi S. Medvedev, Matthew S. Mizuhara, and Andrew Phillips, *A global bifurcation organizing rhythmic activity in a coupled network*, Chaos **32** (2022), no. 8, Paper No. 083116, 13. MR 4465990
- [70] Georgi S. Medvedev and Dmitry E. Pelinovsky, *Turing bifurcation in the Swift-Hohenberg equation on deterministic and random graphs*, J. Nonlinear Sci. **34** (2024), no. 5, 36 (English), Id/No 88.
- [71] Georgi S. Medvedev and Gideon Simpson, *A numerical method for a nonlocal diffusion equation with additive noise*, Stochastics and Partial Differential Equations: Analysis and Computations (2022).
- [72] Georgi S. Medvedev and Xuezhi Tang, *Stability of twisted states in the Kuramoto model on Cayley and random graphs*, J. Nonlinear Sci. **25** (2015), no. 6, 1169–1208 (English).

- [73] ———, *The Kuramoto model on power law graphs: Synchronization and contrast states*, Journal of Nonlinear Science (2018).
- [74] Umberto Mosco, *Analysis and numerics of some fractal boundary value problems*, Boll. Unione Mat. Ital. (9) **6** (2013), no. 1, 53–73 (English).
- [75] H. Neunzert, *Mathematical investigations on particle - in - cell methods*, vol. 9, 1978, pp. 229–254.
- [76] ———, *An introduction to the nonlinear Boltzmann-Vlasov equation*, Kinetic theories and the Boltzmann equation (Montecatini, 1981), Lecture Notes in Math., vol. 1048, Springer, Berlin, 1984, pp. 60–110. MR 740721 (87i:82061)
- [77] Eddie Nijholt and Lee De Ville, *Dynamical systems defined on simplicial complexes: symmetries, conjugacies, and invariant subspaces*, Chaos **32** (2022), no. 9, 20 (English), Id/No 093131.
- [78] S. M. Nikol'skiĭ, *Approximation of functions of several variables and imbedding theorems*, Die Grundlehren der mathematischen Wissenschaften, Band 205, Springer-Verlag, New York-Heidelberg, 1975, Translated from the Russian by John M. Danskin, Jr. MR 0374877
- [79] Robert S. Strichartz, *Differential equations on fractals*, Princeton University Press, Princeton, NJ, 2006, A tutorial. MR 2246975
- [80] Daniel W. Stroock, *Mathematics of Probability*, Grad. Stud. Math., vol. 149, Providence, RI: American Mathematical Society (AMS), 2013 (English).
- [81] Mingsong Yan, Charles Kulick, and Sui Tang, *On the Convergence and Size Transferability of Continuous-depth Graph Neural Networks*, arXiv e-prints (2025), arXiv:2510.03923.